Changes in the properties and distribution of the intermediate and deep waters in the Fram Strait

Helene R. Langehaug[1,2] *and Eva Falck*[3]

[1]*Nansen Environmental and Remote Sensing Center, Bergen, Norway.*
[2]*Bjerknes Centre for Climate Research, Bergen, Norway.*
[3]*Geophysical Institute, University of Bergen, Bergen, Norway.*

Abstract

The Fram Strait is the only deep connection between the Arctic Ocean and the Nordic Seas (Greenland, Iceland, and Norwegian Seas), with a sill depth of approximately 2600 m. Consequently, observations from this area reflect changes in the deep waters of the Arctic Mediterranean. Possible changes in the properties and distribution of the intermediate and deep water masses passing through the Fram Strait have been studied for the period from 1982 to 2008 at a zonal section at 79°N, with special emphasis on the period from 1997 to 2008. The temperature of the Arctic Intermediate Water shows large interannual variability, where the period from 2002 to 2004 was especially cold, indicating a strong winter convection in the Nordic Seas prior to those years. The deep water originating from the Norwegian Sea has become warmer (by about 0.10°C) during the study period. The changes in the properties of the Norwegian Sea Deep Water are caused by changes in its composition, i.e. an increasing fraction of the Eurasian Basin Deep Water and a decreasing fraction of the Greenland Sea Deep Water each year. If this trend continues, the Norwegian Sea Deep Water will have similar characteristics as the Eurasian Basin Deep Water in about 15 years. A prominent feature seen in the ΘS-diagrams from the deep Fram Strait is the disappearance of water with the characteristics of Greenland Sea Deep Water. This very cold water (temperature below -1.1°C) was not observed after 1997, and the minimum temperature in the strait increased by 0.24°C between 1982 and 2008. In the Fram Strait the fraction of intermediate waters has increased, while the fraction of deep waters from the Nordic Seas has decreased. The fraction of deep waters originating from the Arctic Ocean shows no trend.

Keywords: Arctic, Fram Strait, intermediate and deep water masses, *TS*-diagram, mixing triangle, interannual variability.

1. Introduction

The Arctic Ocean and the Nordic Seas form together the Arctic Mediterranean, which is defined as the ocean area north of the Greenland-Scotland Ridge. They are separated from each other by the Greenland-Spitsbergen sill found in the Fram Strait, between Greenland and Svalbard (Fig. 6.1). The sill depth is about 2600 m and the width of the strait is about 600 km at 79°N, but only about 240 km have water depths above 2000 m. The Fram Strait is the only deep connection between the Arctic Ocean and the Nordic Seas and is therefore a suitable place to trace changes in properties of deep waters, originating from the Arctic Ocean and the Nordic Seas.

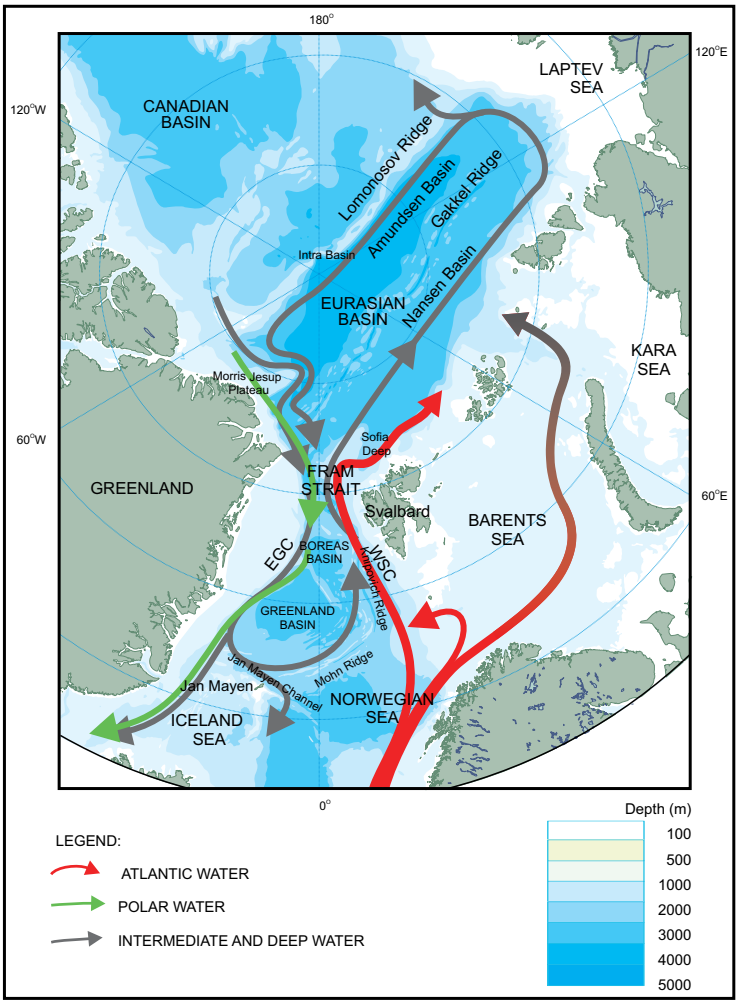

Figure 6.1: Map of the Arctic Mediterranean with bathymetry and main circulation. Abbreviations are: EGC - East Greenland Current; WSC - West Spitsbergen Current.

The Fram Strait is situated between two very different hydrographic regimes, where both the upper and lower water masses show different properties south and north of the sill. The large-scale currents dominating the strait, the West Spitsbergen Current and the East Greenland Current (Fig. 6.1), are mainly topographically steered (Orvik and Niiler, 2002; Nøst and Isachsen, 2003). The water masses transported by these currents meet and interact in the Fram Strait (Rudels et al., 1999). The irregular bathymetry, with troughs, ridges, and seamounts, is one of the factors that generate mixing and a rather complex circulation in the Fram Strait (Clarke et al., 1990; Rudels et al., 1999; Schlichtholz and Houssais, 2002), especially near the sill area.

The Arctic Mediterranean is undergoing observed reduction in the sea ice extent, warmer inflowing Atlantic Water to the Arctic Ocean, and decreased deep water formation in the Greenland Sea. A recent reduction of sea ice extent and thickness in the Arctic, with a record minimum sea ice extent in 2007, has been reported (e.g. Serreze et al., 2007; Comiso et al., 2008; Kwok and Rothrock, 2009). During the last two decades the Atlantic water entering the Arctic Ocean through the Fram Strait has shown an increase in temperature (e.g. Karcher et al., 2003; Maslowski et al., 2004) with a record high temperature in 2006 (Schauer et al., 2008). The deep water production by open ocean convection in the Greenland Sea has weakened since the late 1970s (Rhein, 1991; Schlosser et al., 1991) and it has been shown that the deeper layers of the Greenland Sea are gradually filled with deep waters from the Arctic Ocean, exiting through the Fram Strait (e.g. Meincke and Rudels, 1995). If this situation prevails, the deep waters reaching Fram Strait from the south will contain the slightly modified Arctic Ocean deep waters returning from the Greenland Sea (Rudels et al., 2000).

The West Spitsbergen Current (WSC) flows northward on the eastern side of the Fram Strait (Fig. 6.1), constituting the northernmost extension of the Norwegian Atlantic Current (Aagaard et al., 1987) and carries Atlantic Water into the Arctic Ocean. On the western side of the Fram Strait, the East Greenland Current (EGC) exits the Arctic Ocean (Fig. 6.1) and flows southward. The upper water mass carried by the EGC is the cold and fresh Polar Water from the Arctic Ocean. Several branches of Atlantic Water recirculate from the WSC on its way through the Fram Strait (Aagaard and Coachman, 1968; Bourke et al., 1988). This water, which submerges under the less dense surface water to the west and augments the flow of the EGC, is generally referred to as the Recirculating Atlantic Water. Below the warm and salty Atlantic Water in the WSC, the Arctic Intermediate Water (AIW) and the deep waters arriving from the Nordic Seas, the Norwegian Sea Deep Water (NSDW) and the Greenland Sea Deep Water (GSDW), are found. The water masses originating from the Arctic Ocean, carried by the EGC below the cold and fresh Polar Water, are the Modified Atlantic Water (MAW), the Upper Polar Deep Water (UPDW), the Canadian Basin Deep Water (CBDW), and the Eurasian Basin Deep Water (EBDW).

In a comprehensive water mass analysis based on CTD data collected in 1984, Schlichtholz and Houssais (1999; 2002) defined 12 different water masses between 77 and 81°N. In the present study the same water mass classifications as used by Schlichtholz and Houssais (1999;

2002) have been applied, but only the intermediate and deep waters have been considered. CTD data from the region above the sill at 79°N from the period 1997 to 2008 have been compared with data from the period 1982 to 1988 to analyse how the properties and the distribution of the intermediate and deep waters in the Fram Strait have changed since the mid-1980s. To study changes in the distribution we have used the mixing triangle concept, where we can solve for three water masses. More advanced methods, like the Optimum Multiparameter Analysis (Tomczak and Large, 1989) exist, which can solve the contribution from more than three water masses. These methods require additional parameters, such as nutrients or others.

2. Observations

The observations used in this work are temperature and salinity measurements taken between 1982 and 2008 (Table 6.1). The largest part of the CTD data was obtained from the ICES database (www.ices.dk) and from a CD (Fahrbach, 2006) made in the first phase of the EU project ASOF-N (Arctic/Subarctic Ocean Fluxes North) programme. The accuracy for both temperature and salinity was ± 0.005 during the 1980s and has later improved to ± 0.001°C for temperature and ± 0.003 for salinity (Fahrbach et al., 2007). There are gaps in the CTD data throughout the study period, with the best temporal coverage in 1997-2005. All of the observations used are taken in July, August, and September. The only exception is 1982, when the observations were made in March. The observations downloaded from the ICES database can for one specific year contain observations from more than one cruise.

Table 6.1

Sources for the CTD data

Year	Source	Institute	Research Vessel
1982,1984,1988	ICES	AWI/NPI/IMR/GFI/*	Polarstern/Lance/Johan Hjort
1997-1999	ICES	AWI/NPI/IMR/GFI/*	Polarstern/Lance/Johan Hjort
2001-2005	ASOF-N	AWI/NPI	Polarstern/Lance
2008	-	AWI	Polarstern
1988, 1993**	-	AWI	Polarstern

The abbreviations are as follows: ASOF, Arctic/Subarctic Ocean Fluxes North; ICES, International Council for the Exploration of the Sea; AWI, Alfred Wegener Institute; NPI, Norwegian Polar Institute; IMR, Institute of Marine Research (Norway); GFI, Geophysical Institute (Norway).

*Also contributions from Meteror, Polarsyssel, Oceania, Hudson, Lynch, Valdivia, and Cryos.

** These are bottle data files with temperature and salinity only from depths were the bottle water samples were taken.

The purpose of this work is to investigate water mass properties and distribution above the sill, hence only data from the area 7°W to 9°E and 78.60°N to 79.05°N are considered (Fig. 6.2). In the following, the areas north and south of the sill will be referred to as the northern and southern Fram Strait, respectively.

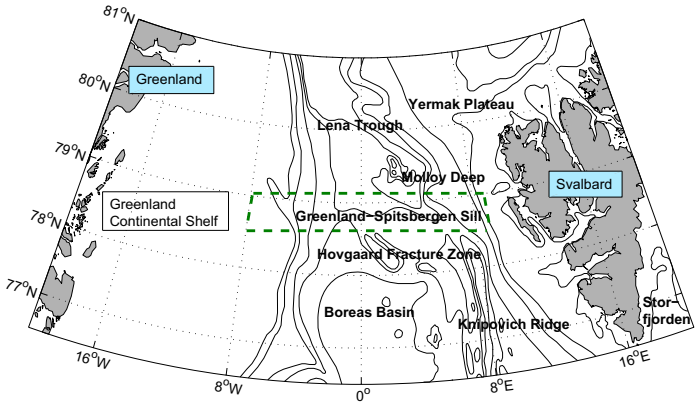

Figure 6.2: Map of the study domain. All data used fall inside the dashed green box, i.e. the area 78.60 -79.05°N and 7°W-9°E. Black contour lines show the bathymetry.

3. Analysis

3.1 ΘS-diagrams

A *TS*-diagram shows the relationship between temperature (or potential temperature, Θ, when deep waters are considered as in this work) and salinity, where different water masses can be identified by their *TS*-properties (Helland-Hansen, 1916). In this work we have adopted the water mass classification used by Schlichtholz and Houssais (1999; 2002), who studied water masses in the Fram Strait, including the northern and southern part, from hydrographic casts taken in summer 1984. The layout of their Θ*S*-diagram is given in Fig. 6.3, where the upper panel shows the full Θ*S*-range for all water masses in the Fram Strait and the lower panel shows the Deep Water (DW) range. In this study we will only use their DW range and investigate the properties of the intermediate and deep waters, where the different water masses are defined by potential temperature and salinity as given in Table 6.2. The DW range in our work includes four deep (Greenland Sea Deep Water (GSDW), Norwegian Sea Deep Water (NSDW), Eurasian Basin Deep Water (EBDW), and Canadian Basin Deep Water (CBDW)) and two intermediate (Arctic Intermediate Water (AIW) and Upper Polar Deep Water (UPDW)) water masses. While Schlichtholz and Houssais (2002) divided the NSDW into a cold (NSDWc) and warm (NSDWw) parts, this study does not explicitly address the latter. Following other authors (e.g. Swift and Koltermann, 1988), we will refer to the NSDWc as NSDW in the rest of our work.

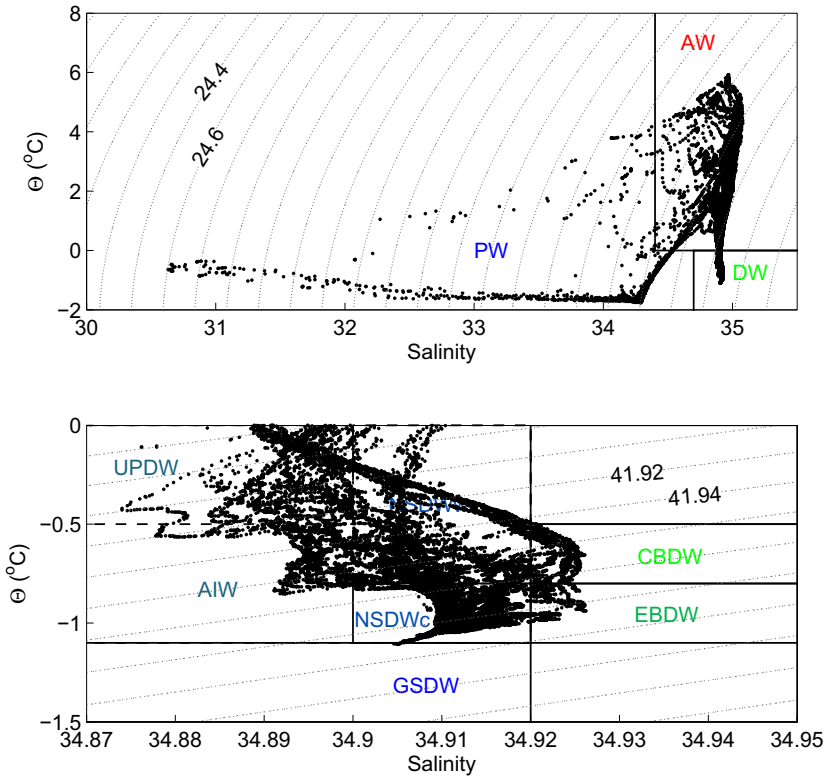

Figure 6.3: The Θ*S*-diagram used in the present analysis is adopted from Schlichtholz and Houssais (2002), and shows here CTD data from 1997. The two Θ*S*-diagrams show the entire Θ*S*-range (upper panel) and the Deep Water range (lower panel). The water mass abbreviations are: PW - Polar Water, AW - Atlantic Water, AIW - Arctic Intermediate Water, UPDW - Upper Polar Deep Water, NSDWw - warm Norwegian Sea Deep Water, CBDW - Canadian Basin Deep Water, NSDWc - cold Norwegian Sea Deep Water, GSDW - Greenland Sea Deep Water, EBDW - Eurasian Basin Deep Water. Dotted isolines show σ_0 (upper panel) and σ_3 (lower panel) surfaces.

Two Θ*S*-diagrams are shown for each year with a sufficient data coverage. To distinguish between spatially different properties of water masses, the observations are presented separately for the eastern and western part of the strait (as divided by the Greenwich meridian).

Table 6.2

Water mass classification (after Schlichtholz and Houssais, 2002)

Acronym[1]	Pot. Temperature [°C]	Salinity	Depth of Core [m]
AIW	-1.1°C<Θ<-0.5°C	34.7<S<34.9	550±200
	-0.8°C<Θ<0°C	34.9<S<34.92[2]	
UPDW	-0.5°C<Θ<0°C	34.7<S<34.9[3]	1008±172
$NSDW_W$	-0.8°C<Θ<-0.5°C	34.9<S<34.92[4]	947±161
	-0.5°C<Θ<0°C	34.9<S<34.92[5]	
CBDW	-0.8°C<Θ<-0.5°C	S>34.92	1500±138
$NSDW_C$	-1.1°C<Θ<-0.8°C	34.9<S<34.92	1610±334
EBDW	-1.1°C<Θ<-0.8°C	S>34.92	2333±303
GSDW	Θ<-1.1°C	34.7<S<34.92	2482±300

[1] AIW-Arctic Intermediate Water, UPDW-Upper Polar Deep Water, $NSDW_W$-warm Norwegian Sea Deep Water, CBDW-Canadian Basin Deep Water, $NSDW_C$-cold Norwegian Sea Deep Water, EBDW-Eurasian Basin Deep Water, GSDW-Greenland Sea Deep Water;

[2] if a salinity minimum is found in the range -1.1°C < Θ < -0.5°C; 34.7 < S < 34.9;

[3] only if the mean ΘS regression slope is negative;

[4] if not AIW;

[5] if not AIW nor UPDW.

3.2 Mixing triangle

In this study we use a mixing triangle (Mamayev, 1975; Tomczak, 1981) to calculate the contributions of the different source water masses. The mixing triangle represents an area in the Θ*S*-diagram, which is spanned by the characteristics of three source water types (corners in the triangle; $\Theta_1 S_1$, $\Theta_2 S_2$, $\Theta_3 S_3$). It is based on the assumptions that the relative contribution of individual source water masses in a water sample can be calculated, since the source water masses to a large extent retain their characteristics when they leave their formation region and remain isolated from the surface. The conservation equations for the conservative properties and mass conservation are used. This implies identical mixing coefficients for all parameters, assuming a dominance of turbulent mixing over other mixing processes. A system of linear equations are used as represented by Equations 6.1-6.3:

$$x_1\Theta_1 + x_2\Theta_2 + x_3\Theta_3 = \Theta_{obs} \tag{6.1}$$

$$x_1 S_1 + x_2 S_2 + x_3 S_3 = S_{obs} \tag{6.2}$$

$$x_1 + x_2 + x_3 = 1 \tag{6.3}$$

where x_1, x_2, and x_3 are the fractions of the three source water types which, due to the mass conservation sum up to 1. Θ_{1-3} and $S_{1-3}$are the temperature and salinity, respectively, of the different source waters and Θ_{obs} and S_{obs} are the observed values. Mixing between three source

water types results in a product with the characteristics $\Theta_{obs}S_{obs}$ that lie within the mixing triangle. Since the number of source water masses is more than three for the deep waters in the Fram Strait, we have combined some of the water masses: The NSDW and the GSDW are combined into the Nordic Seas Deep Water (NDW), and the CBDW and the EBDW into the Arctic Ocean Deep Water (AODW). AIW was chosen as third water mass since it is present on both sides of the Fram Strait. Only data with temperatures below -0.5°C in the DW range are considered. The characteristics of these water masses are given in Table 6.3. The characteristics of NDW and AODW are not simple arithmetic averages of the properties of the respective source water masses (NSDW and GSDW, and CBDW and EBDW), but are calculated according to the formulas given in Table 6.3 which are based on the water mass fractions found in 1984 (see later discussion).

Table 6.3
Source water mass characteristics

Acronym[1]	Θ [°C]	S	Acronym[1]	Θ [°C]	S	Source
AIW	-0.730	34.897				Jeansson et al. (2008)[2]
CBDW[3]	-0.502	34.949	AODW[4]	-0.728	34.932	
EBDW	-0.816	34.929				Swift and Koltermann (1988)
NSDW	-1.048	34.910	NDW[5]	-1.114	34.905	Swift and Koltermann (1988)
GSDW	-1.242	34.895				Swift and Koltermann (1988)

[1] The water mass abbreviations are as follows: AIW, Arctic Intermediate Water; CBDW, Canadian Basin Deep Water; EBDW, Eurasian Basin Deep Water; NSDW, Norwegian Sea Deep Water; GSDW, Greenland Sea Deep Water; AODW, Arctic Ocean Deep Water; NDW, Nordic Seas Deep Water. Θ is potential temperature and S is salinity.

[2] ΘS-properties of their Northern Arctic Intermediate Water.

[3] ΘS-properties are based on a profile taken in 1994 (18SN19940726) in the Canadian Basin, close to the Intra Basin at the Lomonosov Ridge, at depths between 1750-1900 m.

[4] This has been calculated by the following formulae: AODW = 0.5 (0.5 CBDW + 0.5 EBDW*) + 0.5 EBDW, where EBDW* indicate properties taken from the Intra Basin at the same depths as the CBDW.

[5] This has been calculated by the following formulae: NDW = 0.5 (0.4 GSDW + 0.6 EBDW) + 0.5 GSDW.

In this work we have kept the characteristics of the source water masses constant in time (Table 6.3). The constant characteristics of the source waters are appropriate for the deep waters from the Arctic Ocean (CBDW and EBDW) due to their long residence times (Macdonald et al., 2005). Regarding the deep waters from the Nordic Seas, we have used the characteristics of the deep water in the Greenland Sea and the Norwegian Sea as observed in the early 1980s because we are interested in the changes after this time period. AIW is more variable from year to year than the deep waters, depending on the strength of the winter convection. Since we do not know the exact location of its formation, we have chosen to keep the characteristics of AIW constant as for the other water masses.

The mixing triangle, based on the characteristics of AIW, NDW, and AODW (given in Table 6.3), do not cover the total amount of data in the ΘS-diagram (Fig. 6.4). To get an estimate of the validity of the analysis considering the definition of the source water masses we have performed the analysis ten times with changing characteristics of the source water masses. The characteristics were randomly chosen for each time the analysis was run, where one ΘS-value from the intervals $\Theta \pm 0.1$°C and S $\pm$ 0.01 was applied for each source water mass. These intervals have been chosen so that all data in the ΘS-diagram could be covered by the mixing triangle in one or more runs. Θ and S are the potential temperature and salinity, respectively, for each of the source water masses as given in Table 6.3. The mean of the water mass compositions from the ten runs has been used.

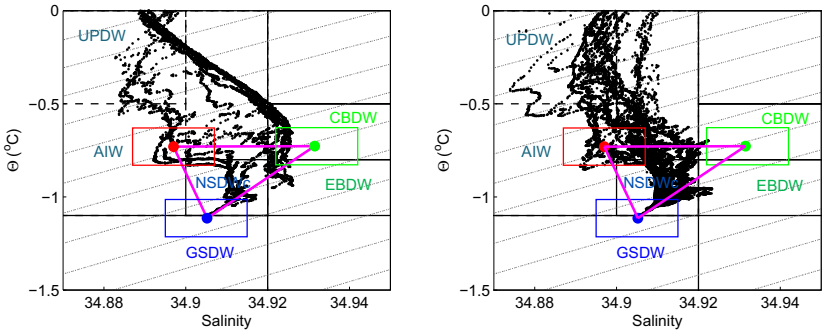

Figure 6.4: ΘS-diagram of the Deep Water range in the Fram Strait, showing the CTD data taken in 1997. The columns (left and right) show observations west and east of the zero meridian, respectively. The mixing triangle is given by the source water mass characteristics denoted by the coloured circles. The coloured boxes indicate the upper and lower boundaries of the respective source values used in the sensitivity analysis. Dotted isolines show σ_3-surfaces.

4. Properties and origin of intermediate and deep water masses

To get an overview of the complex system of the water masses, a conceptual model of the water mass distribution in the 1980s at 79°N in the Fram Strait is presented in Fig. 6.5. The water masses in the eastern part of the strait will mainly follow the WSC northward, while the water masses in the western part flow mainly southward carried by the EGC (Schlichtholz and Houssais, 2002). The flow pattern in the strait is, however, much more complex than this simplified picture suggests, with numerous recirculations south and north of the sill (Aagaard and Coachman, 1968; Bourke et al., 1988). For instance, deep waters from the Nordic Seas may recirculate in the northern Fram Strait towards the western side. The deep waters leaving the Arctic Ocean that are located too deep to pass over the ridge between Greenland and Jan Mayen (i.e. below 1600 m) will circulate around the rim of the Greenland Basin and eventually return back to the Fram Strait.

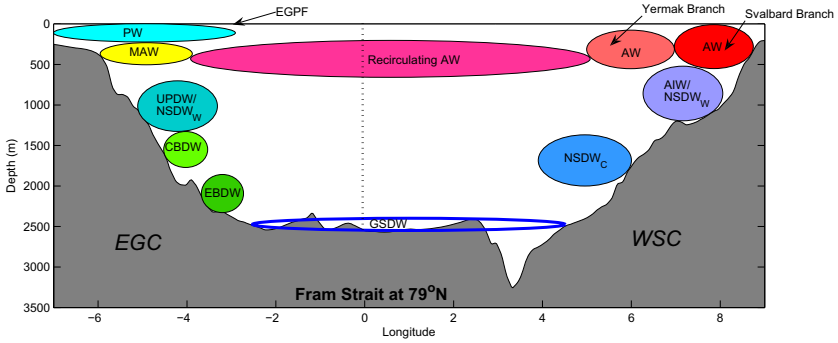

Figure 6.5: A conceptual model of the water mass distribution in the 1980's above the sill in the Fram Strait. Colour shaded circles denote the cores of the different water masses. Cores confined to the east of the zero meridian flow mainly northward in the West Spitsbergen Current (WSC), while the cores confined to the west of the zero meridian flow mainly southward in the East Greenland Current (EGC). The water mass abbreviations are given in Fig. 6.3. The East Greenland Polar Front (EGPF) separates the cold and fresh Polar Water (PW) from the warm and saline Atlantic Water (AW).

Arctic Intermediate Water (AIW) is formed in the Greenland and Iceland Seas by cooling of Arctic Surface Water during winter (Swift, 1986) and sinking to intermediate depths, from where it spreads out over most of the Nordic Seas. The AIW was introduced by Swift and Aagaard (1981) as upper Arctic Intermediate Water. Newly formed AIW shows both a temperature and a salinity minimum, but the temperature minimum disappears as the AIW moves away from its source regions (Rudels et al., 2005). It is transported towards the Arctic Ocean in the eastern part of the strait. The AIW has been identified at the western and northern slopes of the Yermak Plateau (Fig. 6.2) and followed around the plateau into the Sofia Deep (Fig. 6.1), where its presence was fairly weak, indicating extensive mixing with ambient water (Rudels et al., 2000). The AIW is recognized in a ΘS-diagram as a positive slope above the core of the water mass, which can be seen as a salinity minimum in the deep Fram Strait.

Norwegian Sea Deep Water (NSDW) cannot be formed locally by deep convection in the Norwegian Sea, since the winter convection only reaches down to about 300-600 m (Clarke et al., 1990; Nilsen and Falck, 2006), but has to be imported into the area. The NSDW is slightly warmer and more saline than the GSDW and is a mixture of GSDW and EBDW (Aagaard et al., 1985; Swift and Koltermann, 1988). The mixing of GSDW and EBDW starts in the Fram Strait (Aagaard et al., 1991) and continues along the periphery of the Greenland Sea. Eventually, the mixture spills out of the enclosed Greenland Basin, mainly across the 2200 m deep sill in the Jan Mayen Channel (Fig. 6.1), and spreads along the bottom in the Norwegian Sea. After entering the Norwegian Sea this water mass is called NSDW (Swift and Kolterman, 1988).

The NSDW leaves the Norwegian Sea to the north as the lower layer of the WSC (below about 1000 m; Schlichtholz and Houssais, 1999). Some of the NSDW participates in the cyclonic circulation in the Boreas Basin south of the sill (Schlichtholz and Houssais, 1999), while the

rest of the NSDW enters the Fram Strait. A considerable fraction of this recirculates north of the Molloy Deep (Fig. 6.2), while only a small portion continues its northward course into the Arctic Ocean along the western slope of the Yermak Plateau (Schlichtholz and Houssais, 1999). The NSDW has been followed to the northern side of the Yermak Plateau in 1991 (Jones et al., 1995) and into the Sofia Deep in 1997 (Rudels et al., 2000). Thereafter, the signature of the NSDW in the deeper layers of the Arctic Ocean disappears quickly, suggesting that the NSDW cannot be a major contributor to the EBDW (Rudels et al., 2000), although Frank et al. (1998) identified NSDW from tracer distributions as far east as at the Laptev Sea slope (Fig. 6.1).

Greenland Sea Deep Water (GSDW), produced in the Greenland Sea by open ocean convection (Nansen, 1906; Helland-Hansen and Nansen, 1909), is known to form the freshest, coldest, and densest deep water in the Arctic Mediterranean. A considerable reduction in the formation of this deep water has taken place since the late 1970s (Rhein, 1991; Schlosser et al., 1991, Bönisch and Schlosser, 1995), due to a weakened convection in the Greenland Sea. During the 1990s a great change was observed in the Greenland Sea, from doming to a two-layer structure (Meincke and Rudels, 1995; Budéus et al., 1998; Ronski and Budéus, 2005), and the GSDW became isolated from the newly ventilated intermediate waters. The GSDW can only leave the Greenland Sea either to the east, through the Jan Mayen Channel (2200 m), or to the north, through the Fram Strait (2600 m).

Table 6.4
Data used in Figures 6, 7 and 8.

Year	Name of Cruise[1]	Month	Region	Parameters
1982	18HU19820228	March	Nordic Seas	Θ and S
1991	77DN19910726	August-September	Arctic Ocean	Θ and S
1994	18SN19940724	August	Arctic Ocean	Θ and S
1996	06AQ19960712	August-September	Arctic Ocean	Θ and S

Data from:
http://cdiac.ornl.gov/ftp/oceans/CARINA/CARINA_Database/CARINA.AMS.V1.2/
[1]Expocode which consists of two characters identifying the country code followed by the two character vessel NODC (National Oceanographic Data Center) code and the last eight numbers denoting the starting date of the cruise (as YYYYMMDD).

A few observations taken in the Boreas Basin and along the continental slope west of Svalbard (Fig. 6.6) are shown in Fig. 6.7 to get an impression of what typical Θ*S*-profiles look like south of the Fram Strait. The data sources for these profiles are given in Table 6.4. Stations 36, 18, 19, and 50 clearly show GSDW and the black dot indicates the definition of GSDW given by Swift and Koltermann (1988). Stations 51, 52, and 24, which are closest to the continental slope, show only NSDW, with the densest water properties similar to the definition of NSDW given by Swift and Koltermann (1988). The AIW is seen in all Θ*S*-profiles, except station 52, with a much colder salinity minimum in the Boreas Basin than along the continental slope.

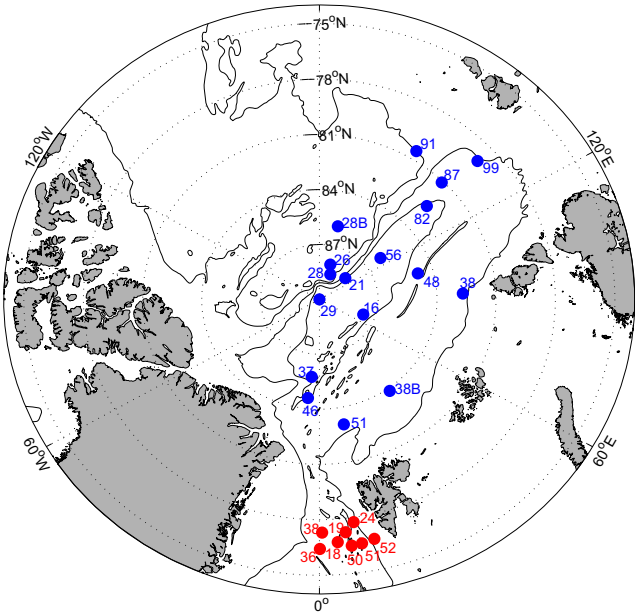

Figure 6.6: Overview of the station positions for the ΘS-profiles shown in Fig. 6.7 and 6.8. Blue dots denote profiles from the Canadian Basin and the Eurasian Basin, while red dots denote profiles from south of the Fram Strait. Data sources are given in Table 6.4.

Upper Polar Deep Water (UPDW) originates in the Arctic Ocean. In the Canadian Basin the UPDW is a product of shelf-slope convection, found between the Atlantic Water and CBDW layers. In the Eurasian Basin the inflow of colder and less saline Atlantic Water from the Barents Sea creates a salinity minimum, and occasionally a temperature minimum, between the Atlantic Layer and the EBDW (Rudels et al., 1999). One can distinguish between UPDW originating from the Canadian and Eurasian Basins (Rudels et al., 1994). For the UPDW derived from the Canadian Basin the ΘS-curves form a straight line while for the outflow from the Eurasian Basin they have a concave shape below the temperature maximum in the Atlantic Layer. The UPDW of the two basins meet north of the Fram Strait and is transported towards the south through the western part of the strait (Rudels et al., 1994). Both types of UPDW were clearly seen in the central parts of northern Fram Strait in the Oden 2002 data, but at 79°N no distinction between the UPDW from the Canadian and Eurasian Basins could be seen (Rudels et al., 2005). Being less dense than the CBDW and the EBDW, the UPDW is the most likely to cross the ridge between Greenland and Jan Mayen (1600 m) and continue southward into the Iceland Sea. The UPDW has been observed in the southern Iceland Sea, leaving the Nordic Seas through the Denmark Strait (Tanhua et al., 2005; Jeansson et al., 2008). The UPDW can be recognized in the ΘS-diagrams from the Fram Strait as a negative slope, extending from the UPDW properties to the CBDW properties.

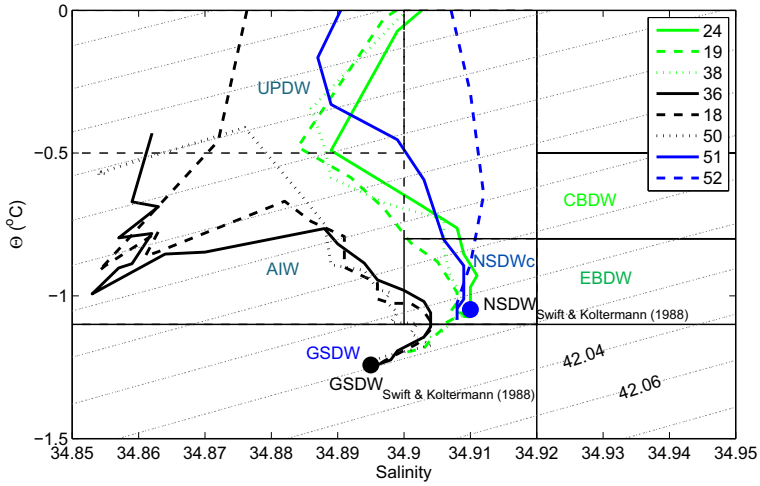

Figure 6.7: ΘS-profiles taken south of the Fram Strait. The station numbers refer to the station numbers given by red dots in Fig. 6.6. The blue and black dots indicate the definition of NSDW and GSDW given by Swift and Koltermann (1988), respectively. Dotted isolines show σ_3-surfaces.

Canadian Basin Deep Water (CBDW) is mostly warmer and more saline water originating from the Eurasian Basin, which was modified there by interactions between dense shelf plumes and the Atlantic derived water (Aagaard et al., 1985; Jones et al., 1995). The exchange of water between the Eurasian and Canadian Basins takes place in the boundary current (Fig. 6.1) along the slope of the Arctic Ocean, but deep water can also cross gaps in the Lomonosov Ridge (e.g. Jones et al., 1995). The CBDW that crosses the Lomonosov Ridge will manifest as a salinity maximum in the Amundsen Basin at about 1700-2000 m (Anderson et al., 1994; Jones et al., 1995; Meincke et al., 1997; Rudels et al., 1999), and can be followed along the northern Greenland slope and into the Fram Strait and the Greenland Sea. A denser fraction of the CBDW will follow the eastward circulation along the southern rim of the Greenland Sea above the EBDW, while the less dense CBDW, if above 1600 m, can continue southwards, between Greenland and Jan Mayen, into the Iceland Sea (Aagaard et al., 1985; 1991). Waters with the characteristics of CBDW have been observed at the sill of the Denmark Strait (Buch et al., 1996), but are generally too dense and located too deep to pass through the Denmark Strait (Buch et al., 1996; Rudels et al., 1999; Jeansson et al. 2008) and hence must flow eastward north of Iceland.

Eurasian Basin Deep Water (EBDW) is essentially a mixture of dense plumes formed on the Arctic shelves and fresher and colder deep water from the Nordic Seas entering trough the Fram Strait (Aagaard et al., 1985), the latter being probably a minor contribution (Jones et al., 1995). Dense plumes entering the deep Eurasian Basin yield the vertical redistribution of heat, producing a bottom layer with relatively constant temperature and salinity increasing with depth (Rudels et al., 1999). Aagaard (1981) and Smethie et al. (1988) pointed out that there are two

distinct water masses in the Eurasian Basin: the EBDW and the Eurasian Basin Bottom Water (EBBW). They showed a clear separation between the two water masses at σ_2 = 37.46, and this interface was found at a depth of about 2500 m, i.e. close to the sill depth of the Fram Strait. The upper part of the EBDW enters the Canadian Basin over the Lomonosov Ridge, with the main exchange presumably taking place in the boundary current along the continental slope (Aagaard, 1989; Woodgate et al. 2001). In the Fram Strait, Schlichtholz and Houssais (1999) found that the major portion of EBDW that reached the sill area recirculated back north in a weak cyclonic circulation. The EBDW that passes the Fram Strait can be followed around the periphery of the Greenland Sea, where it gradually penetrates towards the centre of the gyre circulation and interacts with the GSDW (Rudels et al., 1993: Meincke and Rudels, 1995). The EBDW has been observed in the Iceland Sea in some years (Buch et al. 1996).

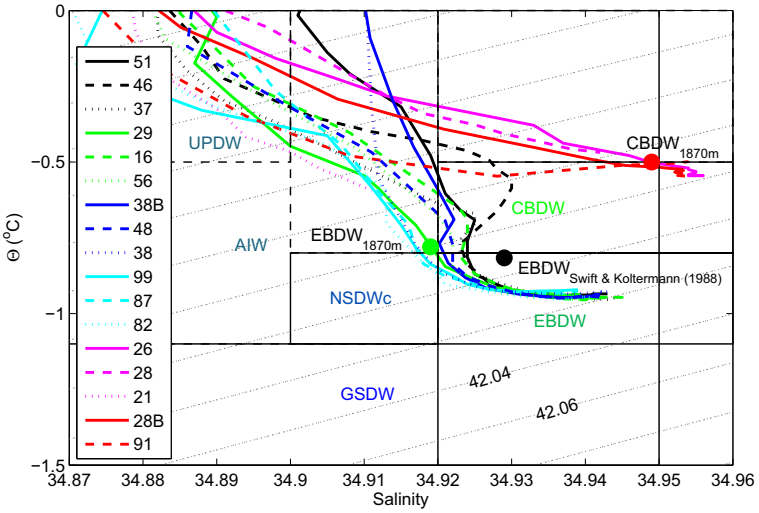

Figure 6.8: Θ*S*-profiles taken in the Canadian Basin and the Eurasian Basin. The station numbers refer to the station numbers given by blue dots in Fig. 6.6. The red and green dots illustrate the Θ*S*-properties measured at a depth of 1870 m, which is the depth of the sill in the Intra Basin. The black dot indicates the definition of EBDW given by Swift and Koltermann (1988). Dotted isolines show σ_3-surfaces.

The characteristics of the water masses originating in the Arctic Ocean are shown in Fig. 6.8. The profiles are taken in the Eurasian Basin and the Canadian Basin (see Fig. 6.6), and the data sources for these profiles are given in Table 6.4. Comparing Θ*S*-profiles from the Eurasian Basin and the Canadian Basin (Fig. 6.8), there is the evident difference between both sides of the Lomonosov Ridge. The CBDW is the saltiest water mass (salinity above 34.95) where its prominent "hook" (Jones et al., 1995) in the deepest part is clearly seen. The EBDW is colder and less saline, with the relatively constant temperature and increasing salinity in the deepest parts. Above these deep waters the UPDW is seen with decreasing temperatures and

increasing salinities (negative slope). The deepest layers of the CBDW are not able to pass into the Eurasian Basin due to the Lomonosov Ridge. It has been assumed that the CBDW enters the Eurasian Basin along the Morris Jesup Plateau (Fig. 6.1) where the deep boundary current meets the different flows recirculating in the Eurasian Basin (Rudels et al., 1999). The Intra Basin (Fig. 6.1), discovered recently in the Lomonosov Ridge (Björk et al., 2007), is a deeper gateway (1870 m) for the CBDW to enter the Eurasian Basin. The maximum depth of this passage is reflected by the depth of intermediate salinity maximum in the Eurasian Basin (about 1800 m; Rudels et al., 1999). This salinity maximum can be identified in several ΘS-profiles from the Eurasian Basin, most pronounced for station 46, but also clearly at stations 37, 16, 48, 51, and 38B. Stations 51 and 38B are found in the Nansen Basin, which means that some of the CBDW enters the Nansen Basin instead of exiting the Fram Strait. Stations 37 and 46 are in route towards Fram Strait and ΘS-profiles similar to these will be what one would expect to see in the western Fram Strait. The red and green dots in Fig. 6.8 show the characteristics of the CBDW and EBDW at their respective sides of the Lomonosov Ridge, at the depth of 1870 m, while the black dot indicates the definition of EBDW given by Swift and Koltermann (1988).

5. Results

The ΘS-diagrams of the DW range express the interannual variability in the ΘS-properties of the different water masses and their presence in the Fram Strait. Two ΘS-diagrams are shown for most of the years presenting properties of the water masses in the eastern and western part of the strait (Fig. 6.9).

A water mass that shows up in some of the ΘS-diagrams, but is not part of this study, is the Storfjorden Plume Water. Storfjorden Plume Water is dense bottom water from Storfjorden in southern Svalbard (Fig. 6.2). It is produced behind the sill of Storfjorden during winter, leaves the fjord and then flows as a dense plume along the continental slope west of Svalbard. In 1986 it was found on the slope at depths between 1000 and 2100 m in the eastern Fram Strait (Quadfasel et al., 1988). In 1988 this water was again observed in the Fram Strait (Schauer, 1995). In the ΘS-diagram for 1988 (Fig. 6.9c) the points forming a positive slope (reaching the upper right corner of the diagram) represent Storfjorden Plume Water. This water is also identified in the ΘS-diagrams in 1998, 2002, and 2008 (Fig. 6.9e, h, l). In some years this signal was not found, due to the absence of a dense water overflow or a lack of observations during the event.

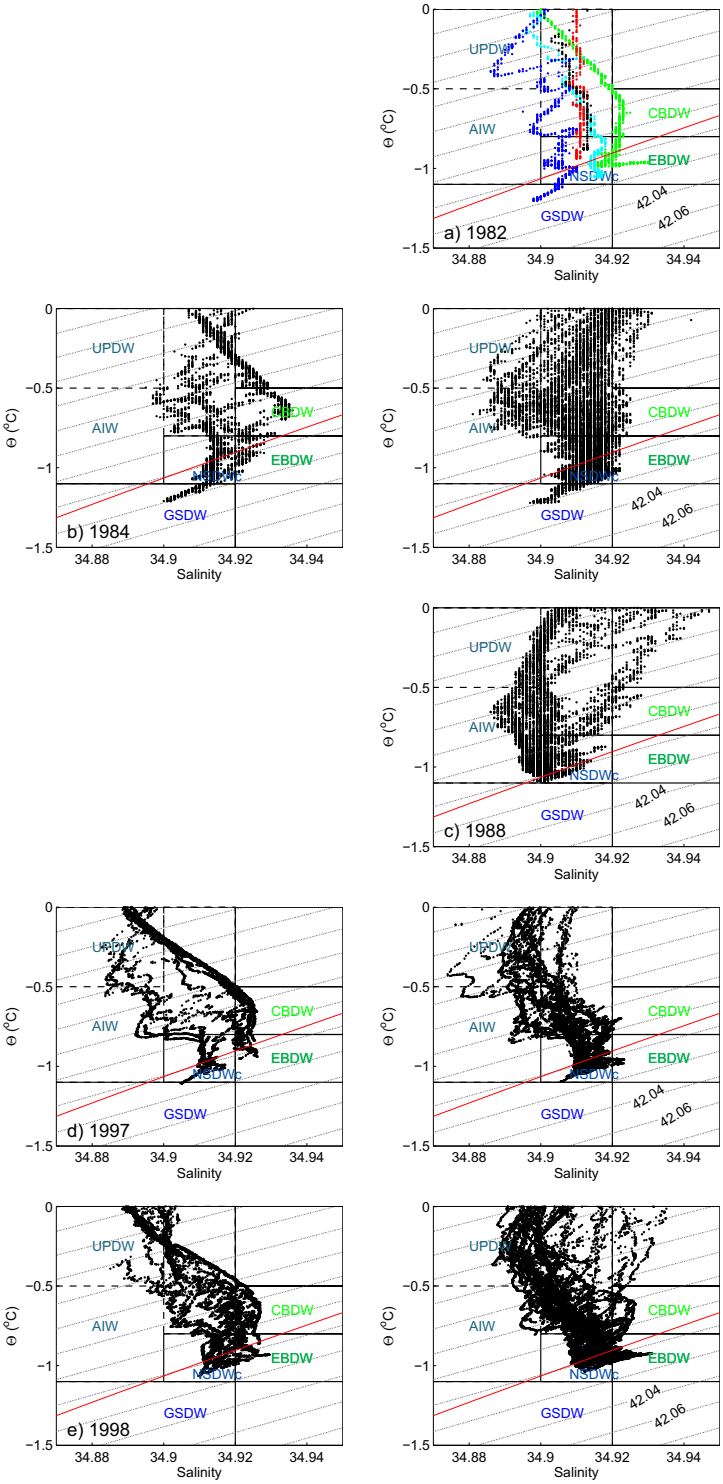
a) 1982
b) 1984
c) 1988
d) 1997
e) 1998
UPDW
AIW
CBDW
EBDW
NSDWc
GSDW
42.04
42.06
Θ (°C)
Salinity
0
−0.5
−1
−1.5
34.88
34.9
34.92
34.94

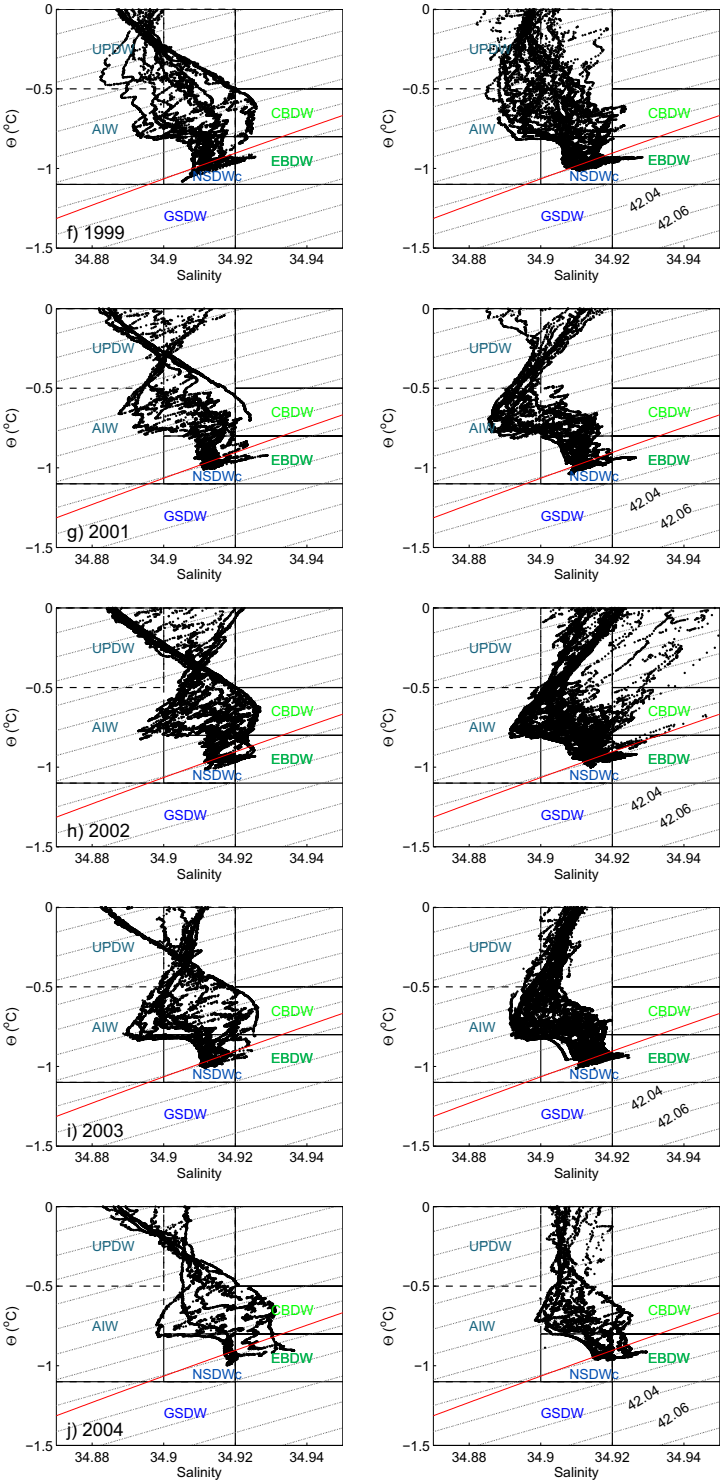
f) 1999
g) 2001
h) 2002
i) 2003
j) 2004
UPDW
AIW
CBDW
EBDW
NSDWc
GSDW
42.04
42.06
Θ (°C)
Salinity
0
−0.5
−1
−1.5
34.88
34.9
34.92
34.94

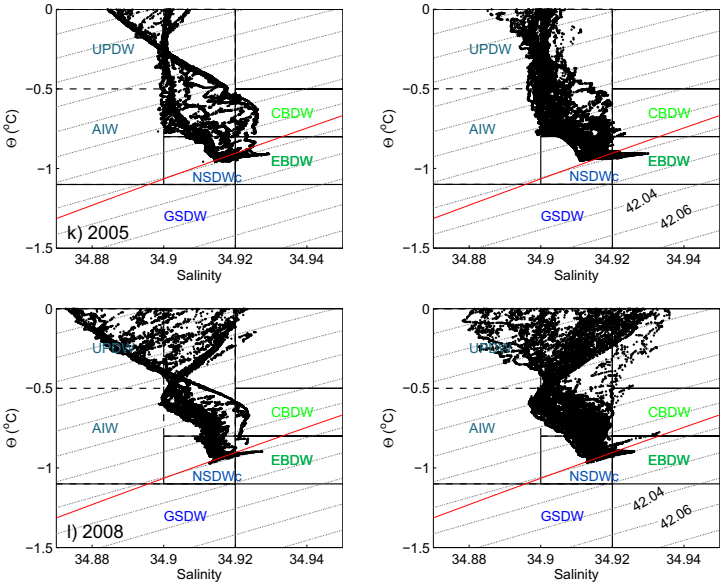

Figure 6.9: ΘS-diagram of the Deep Water range in the Fram Strait, showing the CTD data taken in 1982 (only eastern part), 1984, 1988 (only eastern part), 1997-1999, 2001-2005, and 2008 from top to bottom. The columns (left and right) show observations west and east of the zero meridian, respectively. Dotted isolines show σ_3-surfaces.

Typical profiles representing all deep water masses in the eastern Fram Strait are shown on Fig. 6.9a. The GSDW was observed only at a single profile measured at 5.7°E (blue dots) as a about 500 m thick bottom layer. Above this layer, the lower salinity maximum indicates the NSDW while three salinity minima represent different signals of the AIW. The profile measured at 1.4°E (green dots) reflects the Arctic Ocean derived waters, the UPDW, CBDW, and EBDW with the latter occupying the about 350 m thick bottom layer. Other profiles (red, cyan and black dots) show only the NSDW in the deepest layer.

5.1 Interannual variability of Θ**S-properties of intermediate and deep waters**

Arctic Intermediate Water (AIW) was identified on both sides of the Fram Strait in all years. Both the salinity and temperature in the AIW core changed from year to year, and in many years several salinity minima were seen. Generally, the core with lowest salinity was found in the eastern part of the Fram Strait, except in 2003 and 2004 when it was found in the western part. The depth of this core changed from year to year. In 1984 and 1988 the AIW had a salinity minimum at about 900 m depth, in the eastern Fram Strait, with lowest salinity (34.880) in 1984. From 1997 on the salinity minima were found deeper in the water column, reaching the greatest depth in 2004 on the western side (1250-1400 m), with generally higher salinities than found during the 1980s. In the late 1990s the positive slope above the AIW core is not as clear as in 2001-2003, when the most pronounced signals are seen.

Norwegian Sea Deep Water (NSDW) was also present on both sides of the strait in all years. The NSDW was coldest with temperatures down to -1.1°C in the 1980s, and since then has been gradually warming. Already in 1997 the observations were generally warmer and more saline than in the 1980s, revealing properties more similar to the EBDW, where only a small tail indicate a transition to a colder and less saline water mass (GSDW). The temperature difference between the coldest NSDW and EBDW decreased during the studied period.

Greenland Sea Deep Water (GSDW) was clearly present in the early 1980s on both sides of the strait (at least in 1984). The lowest temperature and salinity values of the GSDW were slightly above -1.2°C and about 34.90, respectively. In 1984 a considerable fraction of the GSDW was found in the bottom layer on both sides of the strait. In 1997 only a small portion of the GSDW was found and afterwards it disappeared completely. The transition between the NSDW and the GSDW can still be seen in 1998 and 1999 on the western side, but not on the eastern side.

Upper Polar Deep Water (UPDW) was observed on the western side in all years, but was mainly absent on the eastern side. The salinity at the upper boundary of the UPWD (corresponding to 0°C isotherm) varied from year to year, with highest salinity in 1984 (>34.9) and lowest in 2008 (<34.88).

Canadian Basin Deep Water (CBDW) was present on both sides in all years, except in 2001 and 2003 when it was not observed on the eastern side. The signal of this water mass was strongest in the western part of the strait during the studied period.

Eurasian Basin Deep Water (EBDW) was present on each side of the strait in all years, except in the eastern part in 1988. In the ΘS-diagram it appears as the water mass with highest salinities, except for the years 1984, 2002, and 2003, when the CBDW had higher salinities. Maximum salinity of EBDW was not constrained to the western Fram Strait, but was in some years found in the eastern part. From 2001 on the EBDW was either the densest water mass

in the Fram Strait or had similar density as the NSDW. Data points with densities above σ_2 = 37.46, which indicate the presence of EBBW in the Fram Strait, was observed in all years, except in 1988 (considering only observations in the eastern strait).

5.2 Spatially averaged Θ**S-properties of water masses**

In Fig. 6.10 the mean temperature and salinity of the different water masses, except the UPDW, for the period from 1997 to 2008 are shown. The calculations were done by taking the mean of all data points falling within each water mass definitions (Table 6.2). Profiles containing Storfjorden Plume Water were removed before averaging. In addition, for each year the minimum temperature in deep waters was plotted together with its corresponding salinity. Also, the salinity corresponding to the zero degree temperature for the UPDW is shown for the western part of the Fram Strait (illustrated as the magenta curve in Fig. 6.10).

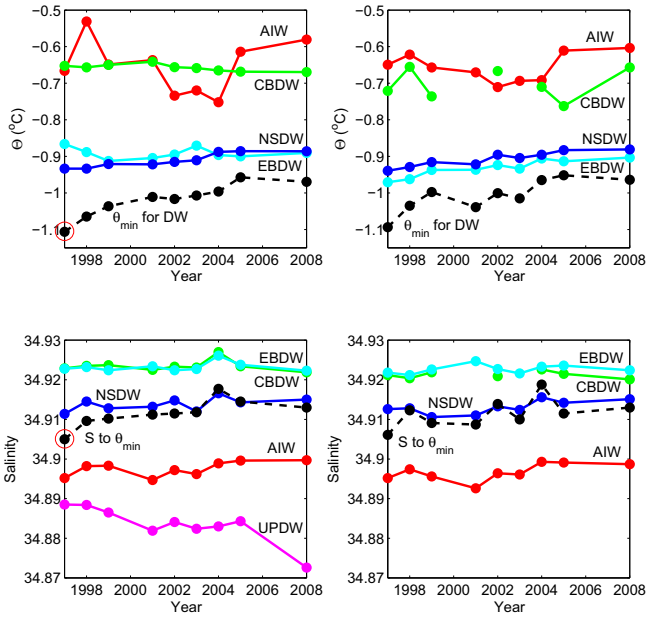

Figure 6.10: Summer mean potential temperature (upper panels) and salinity (lower panels) of the intermediate and deep water masses in the Fram Strait. Dots mark the years with CTD data. Right and left panels are based on observations from east and west of the zero meridian, respectively. The black dashed lines show the minimum potential temperature in the Deep Water range and its corresponding salinity. The red circle denotes the remnants of the GSDW in 1997, concurrent with the minimum potential temperature in the strait. The magenta line in the lower left panel shows the salinity corresponding to the zero degree temperature for the UPDW. Profiles of the Svalbard Plume Water were removed before averaging.

The AIW temperature varied considerably during the period, with high temperature in 1998, rather low between 2002 and 2004, and high again in 2008. The temperature changes from year to year were largest on the western side. Salinity showed moderate interannual variability, and a slightly positive trend can be seen. The mean temperature of the NSDW increased in the western and slightly more in the eastern Fram Strait. The NSDW mean salinity showed small interannual variations and its values were similar on both sides. Remnants of GSDW were only observed in 1997 in the western part and were concurrent with the minimum temperature in the strait that year (illustrated by the red circle in Fig. 6.10). The warmest deep water, the CBDW, varied little throughout the observation period in the western part, both in temperature and salinity. In the eastern part, the changes in temperature were somewhat larger, and in some years the CBDW was not observed at all. The same changes in salinity are seen for both CBDW and EBDW. In the EBDW temperature there was a slight decrease on the western side and an increase on the eastern side. The minimum temperature in the Fram Strait (shown as a black dashed curve in Fig. 6.10) increased by almost 0.14°C and the corresponding salinity increased by about 0.008 (cf. uncertainties described in section 2), assuming that the coldest water was measured. The difference in temperature and salinity between 2008 and 1982 was larger, 0.24°C and 0.015, respectively (not shown). The salinity for the UPDW at zero degree temperature decreased during the period, by about 0.016 (magenta curve in Fig. 6.10).

To look at the general trend in temperature and salinity, without distinguishing between the different water masses, we have used Rudels et al. (2002)'s separation of intermediate and deep waters by the $\sigma_{0.5}$ = 30.444. This makes it possible to include years with sparser data coverage, such as bottle data from 1988 and 1993. For all years properties of water masses denser or lighter than $\sigma_{0.5}$ = 30.444 were averaged together and the mean values are given in Fig. 6.11. The upper panel shows that the temperature of both the intermediate and deep waters were higher in the western compared to the eastern part. The difference in intermediate water temperature between the western and eastern side was largest in the 1980s, but no clear trend is evident. The temperature of deep water reveals a small positive trend during the studied period. The lower panel shows that the salinity of the intermediate water was higher in the 1980s as compared to the later years. The deep waters on the western side were more saline than on the eastern side in the 1980s, but this difference decreased throughout the period, and in 2008 they had similar salinity. The interannual variability was more or less similar for the intermediate and deep waters from 1997 to 2008, and showed concurrent variations in both temperature and salinity.

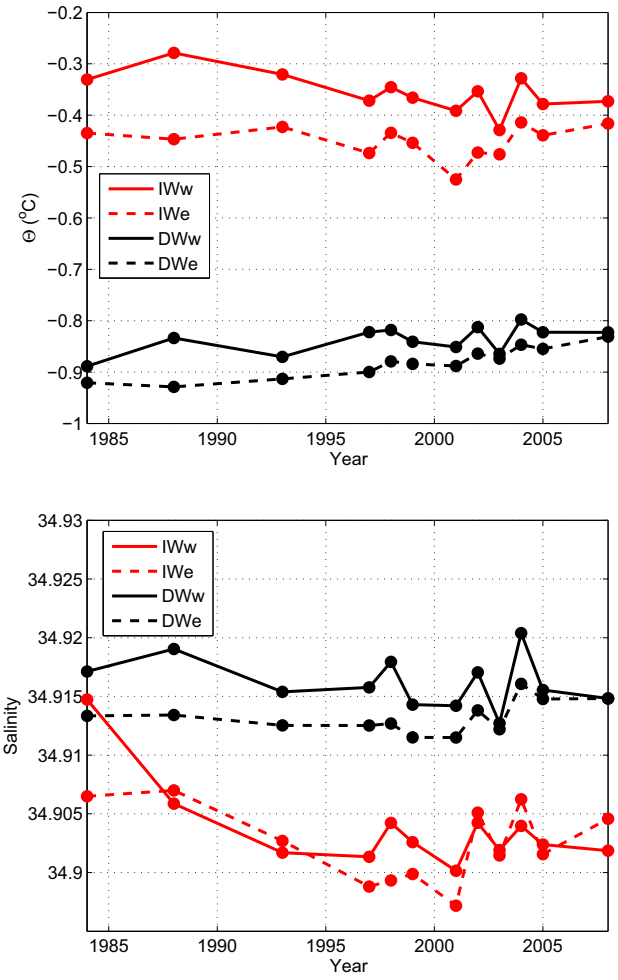

Figure 6.11: Summer mean potential temperature (upper) and salinity (lower) of the intermediate (IW) and deep (DW) waters in the Fram Strait ($\Theta < 0°C$ and $S > 34.87$) for the western (solid line) and eastern (dashed line) side. Rudels et al. (2002)'s separation of IW and DW by the $\sigma_{0.5} = 30.444$ has been used. Dots mark the years with CTD data, except 1988 and 1993 when bottle data have been used. Profiles of the Svalbard Plume Water were removed before averaging.

5.3 Decadal changes

To see the spatial changes in temperature and salinity of the intermediate and deep water over the three decades, vertical sections of temperature and salinity below a depth of 500 m, for the years 1984, 1997, and 2008, are shown in Fig. 6.12. Considerable changes can be seen between 1984 and 2008. The temperature in the deep layers of the Fram Strait has increased; in 1984 the deep waters below about 2000 m were generally colder than -1°C, but in 2008 warmer than -1°C. The -0.8°C isotherm has deepened from about 1300 m to about 2000 m during these years. A clear freshening can be seen between depths of 500-1000 m when comparing 1997 and 1984, and the UPDW at the western edge was particularly fresh in 2008 (as also seen in Fig. 6.10). The high salinity above the continental slope (below 1000 m) shows the outflow of deep water from the Arctic Ocean. In 2008 this high salinity water covered most of the bottom layer, which indicates a change in this layer from fresh and cold GSDW in 1984 to warmer and more saline EBDW in 2008.

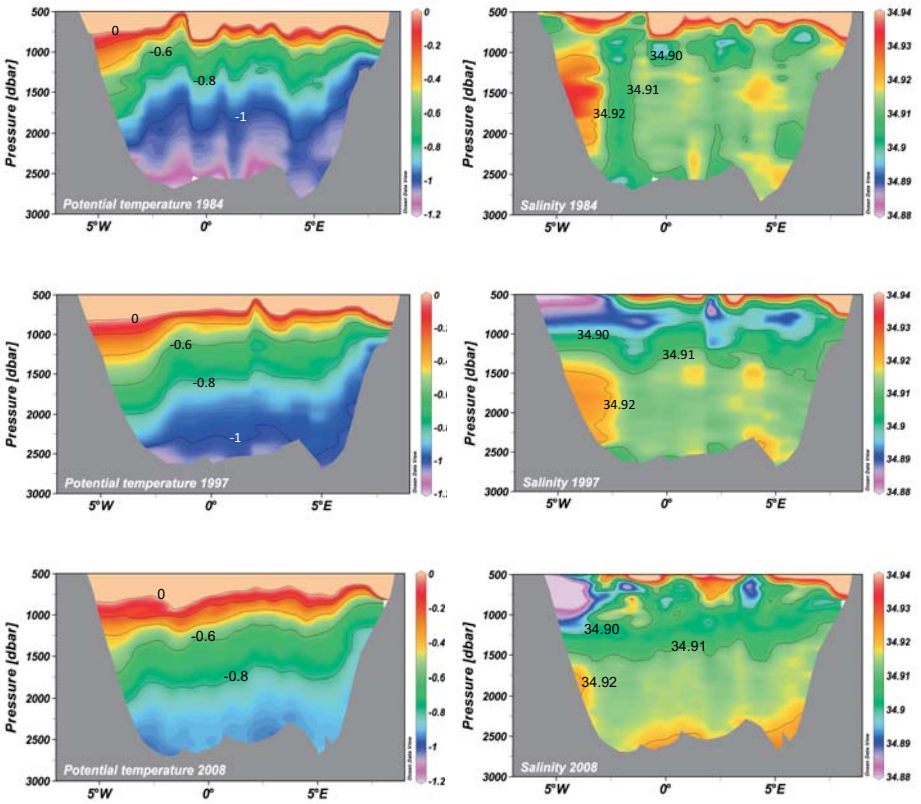

Figure 6.12: Zonal vertical transects of potential temperature (left) and salinity (right) in the Fram Strait in 1984, 1997, and 2008. The grey area shows the bottom. The profiles of Svalbard Plume Water are removed from these plots. The figure is made in Ocean Data View (Schlitzer, 2008).

The mean potential temperature, salinity, and potential density anomaly in 1984, 1997, and 2008 for each of the four deep water masses are given in Table 6.5, together with the total changes (Δ) during the period from 1997 to 2008 and the period from 1984 to 2008. Compared to 1984, the NSDW and the EBDW were warmer both in 1997 and 2008 across the Fram Strait. In the western part there was a significant temperature increase in the NSDW. The rise in temperature resulted in a slight decrease in the density of these water masses while salinity changes were negligible.

Table 6.5

Potential temperature, salinity, and potential density anomaly (σ_3) of the deep water masses in the Fram Strait in 1984, 1997, and 2008.

	West					East				
	1984	**1997**	**2008**	Δ_1	Δ_2	**1984**	**1997**	**2008**	Δ_1	Δ_2
Potential temperature [°C]										
CBDW	-0.628	-0.653	-0.669	-0.016	-0.041	-0.667	-0.721	-0.657	0.064	-0.010
EBDW	-0.895	-0.866	-0.891	-0.025	0.004	-0.980	-0.971	-0.903	0.068	0.077
NSDW	-0.987	-0.934	-0.886	0.048	0.101	-0.968	-0.939	-0.881	0.058	0.087
GSDW	-1.15	-1.11	-	-	-	-1.15	-	-	-	
Salinity										
CBDW	34.931	34.923	34.922	-0.001	-0.009	34.922	34.921	34.920	-0.001	-0.002
EBDW	34.923	34.923	34.922	-0.001	-0.001	34.921	34.922	34.922	0	0.001
NSDW	34.914	34.911	34.915	0.004	0.001	34.913	34.913	34.915	0.002	0.002
GSDW	34.908	34.905	-	-	-	34.905	-	-	-	-
Potential density anomaly [kg/m^3]										
CBDW	41.970	41.967	41.968	0.001	-0.002	41.968	41.974	41.965	-0.009	-0.003
EBDW	41.998	41.994	41.996	0.002	-0.002	42.007	42.006	41.998	-0.008	-0.009
NSDW	42.002	41.993	41.990	-0.003	-0.012	41.999	41.995	41.990	-0.005	-0.009
GSDW	42.017	42.010	-	-	-	42.016	-	-	-	-

Δ_1 is the difference between 2008 and 1997 and Δ_2 between 2008 and 1984. See Table 3 for the water mass abbreviations

Figure 13 presents the layer thickness of the three densest water masses ($\sigma_2 \geq 37.46$) and where in the bottom layer above the sill they are located. Blue dots denote GSDW ($\sigma_2 \geq 37.46$ and $\Theta \leq$ -1.1°C), red dots the densest parts of NSDW ($\sigma_2 \geq 37.46$, $\Theta >$ -1.1°C, and S < 34.92), and green dots EBBW ($\sigma_2 \geq 37.46$ and S $\geq$ 34.92). In 1984 the GSDW was present as a nearly 450 m thick bottom layer in the middle of the strait with NSDW above. The NSDW dominated in the easternmost part, while the largest fraction of EBBW was found at the westernmost station and at one central station. For the period from 1997 to 2008 only NSDW and EBBW were present, except in 1997 when GSDW was found at one station (2°W), with a thickness of about 50 m. The relative fractions of NSDW and EBBW varied during this period with alternating years of predominant NSDW (e.g., 2003) or EBBW (e.g., 2005). Generally, the EBBW, if present, is usually found below the NSDW.

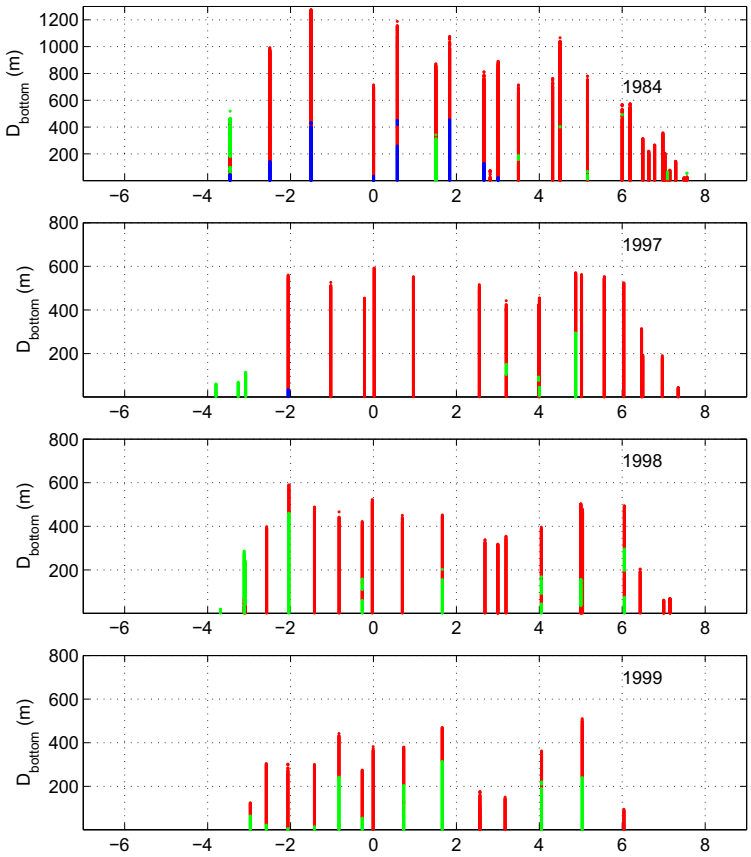

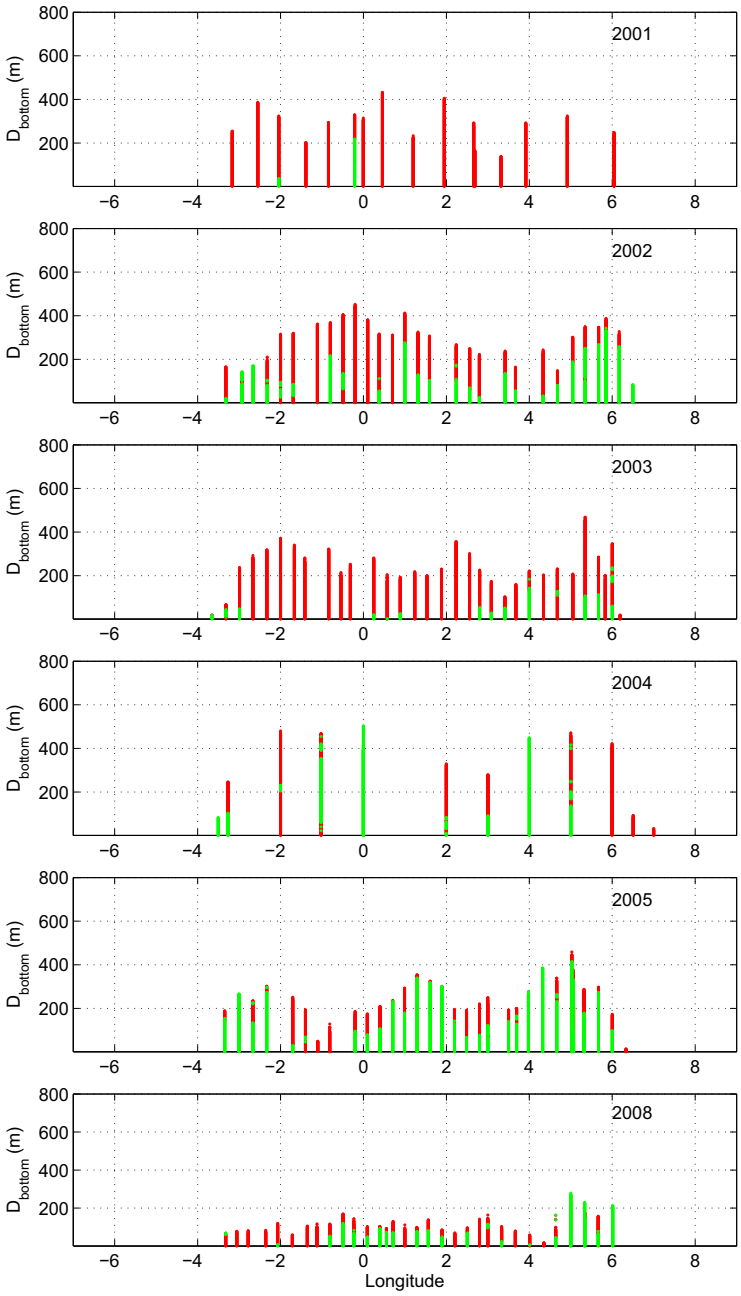

Figure 6.13: Location of waters with the characteristics of GSDW (blue dots), NSDW (red dots), and EBBW (green dots) in the bottom layer above the sill in the Fram Strait. D_{bottom} is the distance from the bottom. The length of the different coloured columns indicates the thickness of each water mass layer. If two stations are close together the dots can appear as overlaid. The data shown here are measured above 2750 m. Note the different scale on the y-axis for year 1984 compared to the other years.

The ΘS-properties of the deep water in the Molly Deep can serve as an indicator of the presence of GSDW north of the sill. Fig. 6.14 demonstrates a change between 1982 and 1997 when the GSDW was found there in the deep water in 1982 and EBDW in 1997, 2004, 2005, and 2008. Schlichtholz and Houssais (2002) observed GSDW also in 1984, when it filled the deepest few hundred meters of the Molloy Deep and EBDW was trapped above, so the change must have occurred after that.

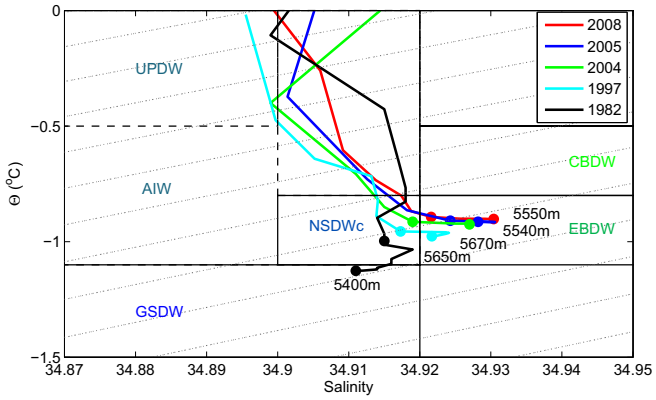

Figure 6.14: ΘS-profiles taken in the Molloy Deep for the years shown in the legend. Two depths are marked for each profile; one with similar depth as the sill in the Fram Strait (2600 m for 1982 and 2500 m for the rest of the years), and one indicating the maximum depth of the profile. Dotted isolines show σ_3-surfaces.

5.4 Variability in the water mass distribution in the deep Fram Strait

The interannual variation in the composition of intermediate and deep water in the Fram Strait is shown in Fig. 6.15. The relative mean errors of these source water fractions (taken as the ratio between the mean fractions and the standard deviations) are rather high (between 23% and 50%). Yet, the trend and the interannual variations are similar for each run, i.e. only the mean fractions vary.

The interannual variability was slightly larger in the western part compared to the eastern part (Fig. 6.15). Table 6.6 shows the fractions of AIW, NDW, and AODW for the different years, together with their means and standard deviations. In the western part about 20% of the waters with Θ < -0.5°C consisted of AIW in 1984, with similar contributions of about 40% from the AODW and NDW. At the end of the studied period the fraction of AIW had increased considerably to nearly 50%, while the greatest reduction was seen in the NDW. Similar changes can also be seen in the eastern part. The largest fraction of AIW was found in 2001, when the AIW core in the Fram Strait was characterized by a pronounced salinity minimum (Fig. 6.9g). The fraction of AODW varied interannually, but showed no trend, with slightly higher fractions

on the western side. The variations in the fraction of AODW on either side of the strait were concurrent with the variations in potential temperature and salinity of the deep waters (black curves in Fig. 6.11). For instance, the largest fraction of AODW was found in 2004, when there was a clear salinity increase for the deep waters.

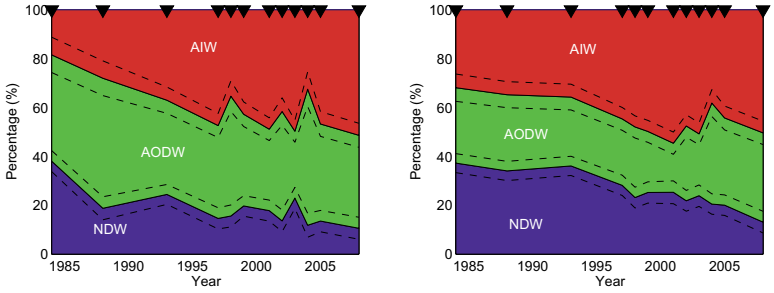

Figure 6.15: Water mass composition from the mixing triangle. Right and left panels are based on observations from east and west of the zero meridian, respectively. The black dashed lines show the 0.5 standard deviation of AIW and NDW fractions. The black triangles indicate the years with CTD data, except 1988 and 1993 when bottle data have been used. Values between the years are interpolations.

Table 6.6

Water mass fractions (%) from the mixing triangle analysis.

	AIW		AODW		NDW	
Year	West	East	West	East	West	East
1984	19	32	43	31	38	37
1988	28	35	53	31	19	34
1993	37	36	39	28	24	36
1997	47	45	38	27	15	28
1998	35	48	49	29	16	23
1999	43	50	38	25	20	25
2001	49	55	33	20	18	25
2002	42	48	45	31	14	22
2003	50	51	27	25	23	24
2004	33	38	56	41	12	20
2005	47	44	40	36	14	20
2008	51	50	38	37	11	13
Mean±std	**40±11**	**44±10**	**42±10**	**30±8**	**18±9**	**26±8**

The last row gives the mean water mass composition for all years and the standard deviations (std).

There was evidently an increase in the relative fraction of intermediate waters and a reduction in deep waters. Fig. 6.16 shows the upper (thin line) and lower (thick line) boundary of the intermediate layer for the years 1984, 1997, and 2008. The boundary between the intermediate and the deep waters ($\sigma_{0.5}$ = 30.444) was much deeper in 2008 compared to 1984, especially on the western side.

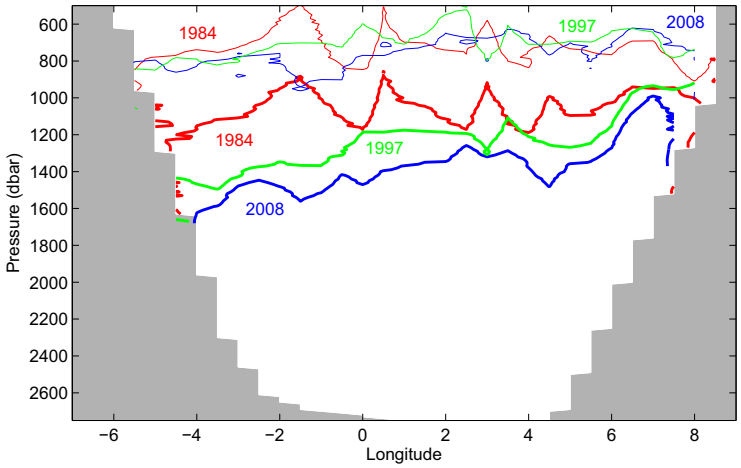

Figure 6.16: Thickness of the intermediate water layer and deep water layer for the years 1984, 1997, and 2008. The intermediate layer is defined as the layer between the 0°C isotherm (thin line) and the $\sigma_{0.5}$ = 30.444 isopycnal (thick line), and deep water is below this isopycnal.

The reduction in the NDW in the Fram Strait is caused by the disappearance of the GSDW and the increasing influence of EBDW in the deep Greenland and Norwegian Seas. To check out this latter assumption on the composition of NSDW, the equations for potential temperature and mass conservation (as shown in Fig. 6.17) have been used. The values for Θ_{GSDW} and Θ_{EBDW} were kept fixed and taken from Swift and Koltermann (1988), while the values used for Θ_{NSDW} are the summer mean potential temperature of NSDW for the different years (as shown in Fig. 6.10). The results are shown in Fig. 6.17. In 1984 the NSDW contained about 40% GSDW and 60% EBDW in the western part and about 35% and 65%, respectively, in the eastern part. In 2008 this had changed to about 15% and 85%, respectively, on both sides. Earlier investigators (Aagaard et al., 1985; Rudels, 1986; Smethie et al., 1988; Swift and Koltermann, 1988) found that the NSDW could be formed from an approximate 1:1 mixture of EBDW and GSDW. This agrees well with our findings for 1984. In the years after, this proportion changed considerably, with an increasing fraction of the EBDW and a decreasing contribution from the GSDW. If the trend shown in Fig. 6.17 continues, i.e. about 1% decrease in the GSDW fraction per year, the NSDW will have similar characteristics as the EBDW in about 15 years. To check the consistency of this trend with the increase in temperature that has been observed in the deep Greenland Sea, we have used the same equations as above, but allowing the properties of

GSDW to change with time. Using the same mixing ratio (GSDW:EBDW) as found in 1984, we see that the temperature in the Greenland Sea must have increased, and in 2008 be slightly above -1°C (Fig. 6.18). This compares well with the findings of Budéus and Ronski (2009), concerning changes in the potential temperature of the deep waters in the Greenland Basin.

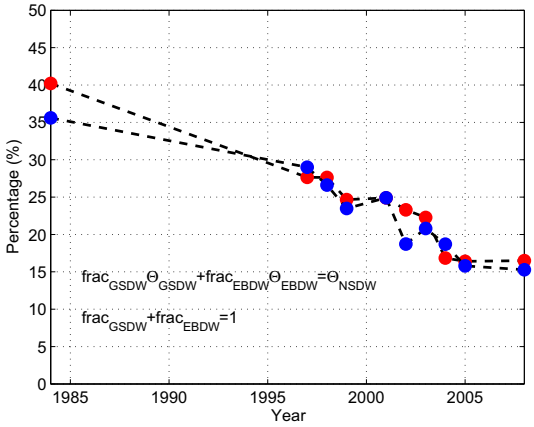

Figure 6.17: Fraction of GSDW in NSDW in the western (red dots) and eastern (blue dots) part of the Fram Strait calculated from the equations given in the figure. The source water mass definitions are taken from Swift and Koltermann (1988), which are given in Table 6.3 and shown as black dots in Fig. 6.7 and 6.8. The values used for Θ_{NSDW} are the summer mean potential temperature of NSDW for the different years (as shown in Fig. 6.10).

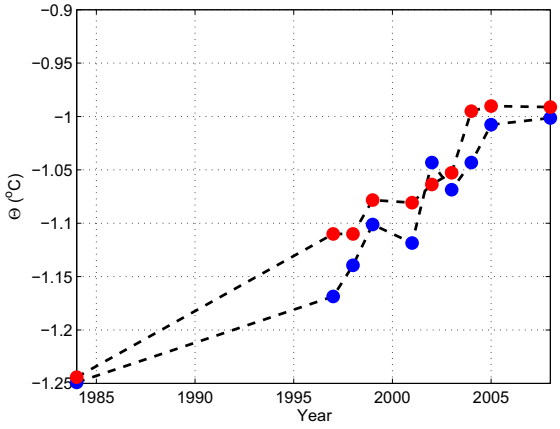

Figure 6.18: Calculated potential temperature of deep water in the Greenland Sea from the equations given in Fig. 6.17 and the fractions from the western (red dots) and the eastern (blue dots) side in 1984.

Although we cannot separate the contribution of CBDW and EBDW by use of the mixing triangle, we can estimate how much the CBDW have been modified on its way from the Canadian Basin to the Fram Strait by mixing with EBDW. The water passing the sill with the strongest remaining characteristics of CBDW is found close to the Greenland continental slope. Hence, we chose one profile from each year at around 4°W (Fig. 6.19) and calculated the relative fractions of CBDW and EBDW in the core of the CBDW (i.e. the salinity maximum) using potential temperature and mass conservation. The fractions were calculated from the potential temperature corresponding to the salinity maximum in the different profiles and the potential temperatures of CBDW and EBDW found at depths of 1870 m close to the Intra Basin. Thus, for these calculations we have assumed that water passing through this gap is the main source of CBDW to the Fram Strait. In 1984 the contribution of CBDW to the salinity maximum observed in the western Fram Strait was 50%. During the period 1997-2008 it varied between 31% (2001) and 59% (1999 and 2005). The mean fraction of CBDW over the whole period was 45%.

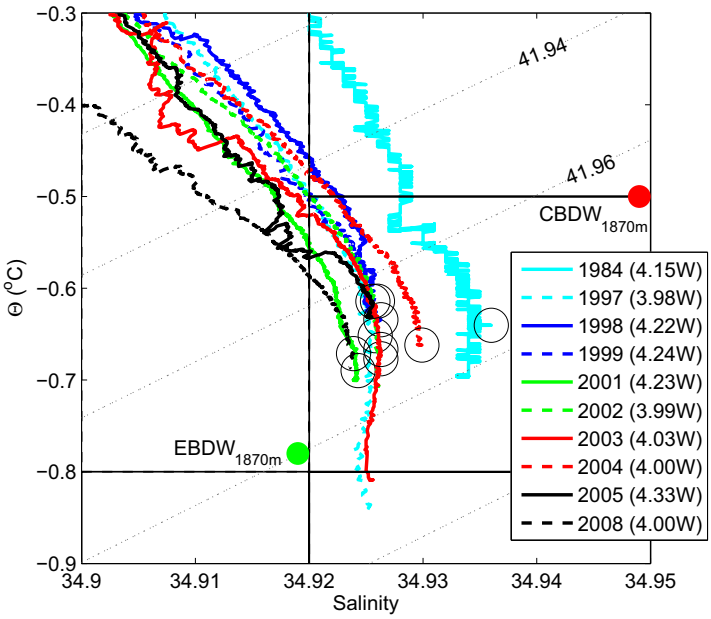

Figure 6.19: Θ*S*-profiles from the western part of the Fram Strait. Year and location of the profiles are shown in the legend. The black circles mark the salinity maximum in each profile. The red and green dots illustrate Θ*S*-properties measured at depths of 1870 m close to the Intra Basin at the Lomonosov Ridge. These properties are used to calculate the relative contribution from CBDW and EBDW to the salinity maxima.

6. Summary and Discussion

Changes in the deep Fram Strait during the last three decades have been revealed in this study:

The **Arctic Intermediate Water** (AIW) showed the greatest interannual variability in potential temperature (Fig. 6.10) of all the water masses considered. The AIW responds directly to the atmospheric forcing in the Nordic Seas and its interannual variability reflects the strength of the winter convection (Swift, 1986). Lowest potential temperature of AIW was found between 2002 and 2004 in the Fram Strait (Fig. 6.10), which coincides with the years of strongest winter convection (down to 1600 m in 2001-2002) observed in the Greenland Sea during the period 1994-2002 (Ronski and Budéus, 2005). In 2003 and 2004 the convection depth in the Greenland Sea decreased again (Budéus and Ronski, 2009), and in 2005 the potential temperature of AIW in the Fram Strait was higher than in 2004. Assuming a time lag for the AIW to reach the Fram Strait, it seems that changes in the Greenland Sea convection can explain the variations in the AIW potential temperature.

Both the salinity in the AIW core and the depth of the core showed an increasing trend. The salinity of the AIW core depends on the salinity of the surface water in the region where it was formed. For instance, both AIW formed in the Boreas Basin and in the Greenland Basin will pass through the Fram Strait, but their respective cores will most probably show different ΘS-properties due to different mixing history and travel time to the Fram Strait (Rudels et al., 1999). This explains the differences between two profiles in the AIW of different origin and also profiles with several salinity minima observed in one individual year (the latter is illustrated by the blue profile in Fig. 6.9a). The AIW was clearly seen in both the western and eastern part, indicating that a significant part of the AIW recirculates at or north of the sill in the Fram Strait. The thickness of this water mass layer increased, and hence, its relative contribution to the deep waters increased from 20-30% in 1984 to 50% in 2008. This increase can be explained by a weaker convection in the Greenland Sea that lead to a higher production of AIW (Rudels et al., 1999; Blindheim and Rey, 2004). It is known that in the Greenland Sea the convection has for many years only ventilated the intermediate waters (Budéus et al. 1998; Ronski and Budéus, 2005; Budéus and Ronski, 2009).

The **Norwegian Sea Deep Water** (NSDW) was characterized by similar interannual variability on both sides of the strait and revealed the largest temperature change of about 0.1°C in 1984-2008 (Table 6.5 and Fig. 6.10). The changes in the ΘS-properties of the NSDW were caused by changes in its composition, with a decreasing fraction of GSDW over the years. This trend, if continues, will result in the NSDW with properties similar to the EBDW in about 15 years. Karstensen et al. (2005) showed that a similar change is taking place in the Greenland Sea and that the GSDW there will reach the AODW characteristics in roughly 20 years (i.e. in 2025) unless new deep water is produced in the Greenland Sea.

The **Greenland Sea Deep Water** (GSDW) was present above the sill in 1982 and 1984 (Fig. 6.9a, b), in some parts of the strait as a nearly 500 m thick bottom layer, but was not found in 1988 (considering only observations for the eastern strait). Coachman and Aagaard (1974) found the GSDW at one station in the Fram Strait while Swift et al. (1983) reported an approximately 100 m thick layer of GSDW, spreading northward along the bottom in 1981. However, Swift et al. (1983) emphasized that they could not determine whether this was a permanent feature or a short-lasting event. Schlichtholz and Houssais (2002) observed that the GSDW was almost exclusively found south of the sill in 1984, in the Boreas Basin, and the model by Bönisch and Schlosser (1995) did not support any significant flow of GSDW into the Arctic Ocean either. Neither did Anderson and Jones (1986) find any direct evidence of the presence of GSDW on the northern slope of the Yermak Plateau, using data from 1981. According to these authors the fraction of northward flowing GSDW was either very small or recirculated in the Fram Strait. From the measurements taken in the Molloy Deep (Fig. 6.14) it is clear that GSDW did pass to the north of the sill at least in 1982.

The last signal of GSDW found in the data used here, was seen in 1997, but only in a very thin bottom layer (50 m) at one station in the western part. After that, no water with the characteristics of GSDW was found above the sill. However, the remnants of GSDW could still be seen in the western part of the strait in 1998 and 1999. Assuming that this water had recirculated north of the sill, this would indicate a period of up to two years for the GSDW to exit again on the western side. The reduction in the formation of the GSDW started between 1978 and 1982 according to Bönisch and Schlosser (1995). In the absence of deep convection, the GSDW will be diluted and slowly removed by turbulent mixing (Meincke et al., 1997; Rudels et al, 1999), and, when the salinity maximum of the AODW finally reaches the bottom, the GSDW will disappear completely.

The **Upper Polar Deep Water** (UPDW) was present in the western part of the strait in all years, but was mainly absent on the eastern side. This is a strong indication that most of the UPDW is situated in the water column shallow enough to exit the Greenland Sea, between Jan Mayen and Greenland (1600 m), and continue southward along the continental slope of the Iceland Sea towards the Denmark Strait. In the Fram Strait it is evident from Fig. 6.16 that the lower boundary of the intermediate waters is located above 1600 m. The presence of UPDW in the Iceland Sea is in accordance with the findings of Olsson et al. (2005), who found that the densest water observed in the Denmark Strait in 1999 was a mixture of UPDW and AIW, with the first being the more important one. Jeansson et al. (2008) also found that UPDW contributed to the densest water at the Denmark Strait sill in 2002. The salinity of UPDW gradually decreased, where the largest change in the salinity occurred between 2005 and 2008. The particularly fresh UPDW in 2008 is evident in Fig. 6.12.

The **Canadian Basin Deep Water** (CBDW) was present in both the western and eastern part (except in 2001 and 2003) of the strait, and its temperature and salinity were highest close to the Greenland continental slope. The CBDW is modified on its way from the Canadian Basin

to the Fram Strait by mixing with EBDW. The averaged fraction of the source CBDW in its diluted core observed in the Fram Strait (i.e. the salinity maximum found close to the Greenland continental slope) for the period from 1984 to 2008 was 45%. Anderson et al. (1994) found that at the Morris Jesup Plateau (Fig. 6.1) the CBDW appeared to be diluted to 50% by EBDW if isopycnal mixing was assumed, while in the central Amundsen Basin the fraction of CBDW was further reduced to about 25%. Rudels (1986) estimated the ratio of CBDW and EBDW in the core of the CBDW (the salinity maximum) to be 1:2 in the Fram Strait. The lack of CBDW in the eastern strait in 2001 and 2003 indicates that in some years all of the CBDW can pass over the Greenland-Jan Mayen Ridge and enter the Iceland Sea. CBDW has been observed in the Iceland Sea, as mentioned in Section 4.1.

The **Eurasian Basin Deep Water** (EBDW) was present in all years in both the eastern (except in 1988) and western parts of the strait. It appears in the ΘS-diagram as the water mass with the highest salinity, with the exception in the western strait for 1984, 2002, and 2003, when the CBDW was more saline. Several years showed a saltier EBDW on the eastern side as compared to the western side, which could indicate an inflow from the north also on the eastern side. Several authors have indicated a southeastward outflow from the Arctic Ocean between the Molloy Deep and the Hovgaard Fracture Zone (Fig. 6.2; Koltermann, 1985; Rudels, 1987; Jónsson and Foldvik, 1992). From 2001 the EBDW was either the densest water mass in the Fram Strait or had similar density as the NSDW.

The presence of EBBW was evident in all years between 1997 and 2008. The EBBW was also found in 2002 by Rudels et al. (2005) at all deep stations in the western Fram Strait at 79°N. On the other hand, in 1988 the EBBW was not found and only barely in 1984. Smethie et al. (1988) and Jones et al. (1991), who used data from 1984 and 1987, respectively, did not find EBBW south of the sill. Schlichtholz and Houssais (2002), also using data from 1984, found the EBBW only north of the sill (in the Lena Trough; Fig. 6.2). Interestingly, the EBBW was observed in 1982 (green profile in Fig. 6.9a), which means that the outflow of EBBW through the Fram Strait is not a recent phenomenon, but can have been a more intermittent incident before the mid 1990s. The EBBW presumably flows southwards along the seafloor in the Lena Trough towards the Molloy Deep, where it circulates around the periphery and, depending on the depth of density interface, either is deflected back north or flows across the sill in the Fram Strait. With the absence of the GSDW at and north of the sill, the possibility of the EBBW to flow over the sill has now increased.

The observed changes in the properties and distributions of the intermediate and deep waters in the Fram Strait may have consequences for the deep circulation in the Arctic Mediterranean. Changes in temperature and salinity (if they do not compensate each other in density) will affect the pressure gradients that influence the exchanges between different basins (e.g., Østerhus and Gammelsrød, 1999; Karcher et al. 2011). What the circulation will look like if all of the deep waters end up having the same properties, as the AODW, is an open question. However, the formation of GSDW may increase again in the Greenland Sea. Deep convection in the Green-

land Sea is assumed to correlate with the variability of the atmospheric pattern that is associated with the North Atlantic Oscillation (NAO), and to be strongest during the negative phase of NAO (Dickson et al., 1996).

Acknowledgments

Many thanks to Agnieszka Beszczynska-Möller, Alfred Wegener Institute, for letting us use the 2008 Polarstern cruise data, which were collected in the frame of the EU DAMOCLES Integrated Project, and the ASOF-N data. The 2003-2005 data were obtained with the support from the EU ASOF-N project (contract No: EVK2-CT-2002-00139) while observations in 2001 and 2002 were supported with the German national funding. We are also very grateful for the comments from two anonymous reviewers that greatly have improved the manuscript. This work has been supported by the Research Council of Norway through the BIAC project (H. R. L.). The authors thank Emil Jeansson, Kjetil Våge, Tor Eldevik, and Svein Østerhus for helpful discussion and comments. This publication is no. XXXX from the Bjerknes Centre for Climate Research.

References

Aagaard, K., 1981. On the deep circulation in the Arctic Ocean. Deep-Sea Res. 28, 251-268.

Aagaard, K., 1989. A synthesis of the Arctic Ocean circulation. Rapp. P.-v. Réun. Cons. Int. Explor. Mer 188, 11-22.

Aagaard, K., Coachman, L.K., 1968. The East Greenland Current north of Denmark Strait: Part II. Arctic 21, 267-290.

Aagaard, K., Foldvik, A., Hillman, S.R., 1987. The West Spitsbergen Current: Disposition and water mass transformation. J. Geophys. Res. 92, 3778-3784.

Aagaard, K., Swift, J.H., Carmack, E.C., 1985. Thermohaline circulation in the Arctic Mediterranean Seas. J. Geophys. Res. 90, 4833-4846.

Aagaard, K., Fahrbach, E., Meincke, J., Swift, J.H., 1991. Saline outflow from the Arctic Ocean: Its contribution to the Deep Waters of the Greenland, Norwegian, and Iceland Seas. J. Geophys. Res. 96, 20433-20441.

Anderson, L.G., Jones, E.P., 1986. Water masses and their chemical constituents in the western Nansen Basin of the Arctic Ocean. Oceanol. Acta 9, 277-283.

Anderson, L.G., Bjork, B., Holby, O., Jones, E.P., Kattner, G., Koltermann, K.P., Liljeblad,

B., Lindegren, R., Rudels, B., Swift, J.H., 1994. Water masses and circulation in the Eurasian Basins: Results from the Oden 91 expedition, J. Geophys. Res. 99 (C2), 3273- 3283.

Björk, G., Jakobsson, M., Rudels, B., Swift, J.H., Anderson, L., Darby, D.A., Backman, J., Coakly, B., Winsor, P., Polyak, L., Edwards, M., 2007. Bathymetry and deep water exchange across the central Lomonosov Ridge at 88-89°N. Deep-Sea Res. I 54, 1197-1208.

Blindheim, J., Rey, F., 2004. Water-mass formation and distribution on the Nordic Seas during the 1990s. J. Mar. Sci. 61, 846-863. doi:10.1016/j.icesjms.2004.05.003.

Bönisch, G., Schlosser, P., 1995. Deep water formation and exchange rates in the Greenland/Norwegian seas and the Eurasian Basin of the Arctic Ocean derived from tracer balances. Prog. Oceanogr. 35, 29-52.

Bourke, R.H., Weigel, A.M., Paquette, R.G., 1988. The westward turning branch of the West Spitsbergen Current. J. Geophys. Res. 93, 14065-14077.

Buch E., Malmberg S.-A., Kristmannsson S.S., 1996. Arctic Ocean deep watermasses in the western Iceland Sea, J. Geophys. Res. 101, 11965-11973.

Budéus, G., Ronski, S., 2009. An Integral View of the Hydrographic Development in the Greenland Sea Over a Decade. The Open Oceanography Journal 3, 8-39.

Budéus, G., Schneider, W., Krause, G., 1998. Winter convection events and bottom water warming in the Greenland Sea. J. Geophys. Res. 103 (C9), 18513-18527.

Clarke, R.A., Swift, J.H., Reid, J.L., Koltermann, K.P., 1990. The formation of Greenland Sea Deep Water: double diffusion or deep convection? Deep-Sea Res. 37, 1385-1424.

Coachman, L.K., Aagaard, K., 1974. Physical oceanography of arctic and subarctic seas. In: Herman, Y. (Eds.), Marine Geology and Oceanography of the Arctic seas. Springer-Verlag, New York, pp. 1-81.

Comiso, J.C., Parkinson, C.L. , Gersten, R., Stock, L., 2008. Accelerated decline in the Arctic sea ice cover. Geophys. Res. Lett. 35, L01703, doi: 10.1029/2007GL031972.

Dickson, R., Lazier, J., Meincke, J., Rhines, P., Swift, J., 1996. Long-term coordinated changes in the convective activity of the North Atlantic. Prog. Oceanogr. 38, 241-295.

Fahrbach, E. (Ed.), 2006. ASOF-N: Arctic-Subarctic Ocean Flux Array for European Climate: North; Contract No: EVK2-CT-2002-00139. Final Report. http://hdl.handle.net/10013/epic.32318.

Fahrbach, E., Rohardt, G., Sieger, R., 2007. 25 Years of Polarstern Hydrography (1982-2007). WDC-MARE Reports 0005, ISSN 1862-4022.

Frank, M., Smethie Jr., W.M., Bayer, R., 1998. Investigation of subsurface water flow along the continental margin of the Eurasian Basin using transient tracers tritium, 3He, and CFCs. J. Geophys. Res. 103, 30773-30792.

Helland-Hansen, B., 1916. Nogen hydrografiske metoder. Forhandlinger ved de skandinaviske Naturforskeres 16de møte, Kristiania, pp. 357-359. (in Norwegian)

Helland-Hansen, B., Nansen, F., 1909. The Norwegian Sea. Its physical oceanography based upon the Norwegian researches 1900-1904. Rep. Norw. Fishery Mar. Invest. 2, pp. 390.

Jeansson, E., Jutterström, S., Rudels, B., Anderson, L.G., Olsson, K.A., Jones, E.P., Smethie, W.M., Swift, J.H., 2008. Sources to the East Greenland Current and its contribution to the Denmark Strait Overflow. Prog. Oceanogr. 78, 12-28.

Jones, E.P., Anderson, L.G., Wallace, D.W. R., 1991. Tracers of near-surface, halocline and deep waters in the Arctic Ocean: Implications for circulation. J. Marine Syst. 2, 241- 255.

Jones, E.P., Rudels, B., Anderson, L.G., 1995. Deep waters of the Arctic Ocean: origins and circulation. Deep-Sea Res. 41, 737-760.

Jónsson, S., Foldvik, A., 1992. The transport and circulation in Fram Strait. ICES CM, 1992/C:10.

Karcher, M.J., Gerdes, R., Kauker, F., Köberle, C., 2003. Arctic warming: Evolution and spreading of the 1990s warm event in the Nordic seas and the Arctic Ocean. J. Geophys. Res. 108(C2), 3034, doi:10.1029/2001JC001265, 2003.

Karcher, M., Beszczynska-Möller, A., Kauker, F., Gerdes, R., Heyen, S., Rudels, B., Schauer, U., 2011. Arctic Ocean warming and its consequences for the Denmark Strait overflow. J. Geophys. Res. 116, C02037, doi 10.1029/2010JC006265.

Karstensen, J., Schlosser, P., Wallace, D.W.R., Bullister, J.L., Blindheim, J., 2005. Water mass transformation in the Greenland Sea during the 1990s. J. Geophys. Res. 110 (C07022), doi: 10.1029/2004JC002510.

Koltermann, K.P., 1985. New evidence for a deep boundary current of polar origin through Fram Strait. ICES CM, 1985/C:38.

Kwok, R., Rothrock, D.A., 2009. Decline in Arctic sea ice thickness from submarine and

ICESat records: 1958 - 2008. Geophys. Res. Lett. 36, L15501, doi: 10.1029/2009GL039035.

Macdonald, R.W., Harner, T., Fyfe, J., 2005. Recent climate change in the Arctic and its impact on contaminant pathways and interpretation of temporal trend data. Sci. Total Environ. 342, 5-86, doi:10.1016/j.scitotenv.2004.12.059.

Mamayev, O.I., 1975. Temperature-Salinity Analysis of World Ocean Water. Elsevier, Amsterdam, pp. 250.

Maslowski, W., Marble, D., Walczowski, W., Schauer, U., Clement, J.L, Semtner, A.J, 2004. On climatological mass, heat, and salt transports through the Barents Sea and Fram Strait from a pan-Arctic coupled ice-ocean model simulation. J. Geophys. Res. 109, C03032, doi:10.1029/2001JC001039.

Meincke, J., Rudels, B., 1995. Greenland Sea Deep Water: A balance between convection and advection. Nordic Seas Symposium, Hamburg, March 1995. Extended Abstract Vol., University of Hamburg, pp. 143-148.

Meincke, J., Rudels, B., Friedrich, H.J., 1997. The Arctic Ocean-Nordic Seas thermohaline system. ICES J. Mar. Sci. 54, 283-299.

Nansen, F., 1906. Northern waters: Captain Roald Amundsen's oceanographic observations in the Arctic seas in 1901. Vid. Selskap. Skrifter, I, Matt.-Naturv. Kl. 1 (3), pp. 145.

Nilsen, J.E.Ø., Falck, E., 2006. Variations of mixed layer properties in the Norwegian Sea for the period 1948-1999. Prog. Oceanogr. 70, 58-90.

Nøst, O.A., Isachsen, P.E., 2003. The large-scale time-mean ocean circulation in the Nordic Seas and Arctic Ocean estimated from simplified dynamics. J. Mar. Res. 61 (2), 175-210.

Olsson, K.A., Jeansson, E., Tanhua, T., Gascard, J.-C., 2005. The East Greenland Current studied with CFCs and released sulphur hexafluoride. J. Marine Syst. 55, 77-95.

Orvik, K. A., Niiler, P., 2002. Major pathways of Atlantic water in the northern North Atlantic and Nordic Seas toward Arctic. Geophys. Res. Lett. 29 (19), 1896, doi:10.1029/2002GL015002.

Østerhus, S., Gammelsrød, T. 1999. The Abyss of the Nordic Seas is Warming. J. Clim. 12 (11), 3297-3304.

Quadfasel, D., Rudels, B., Kurz, K., 1988. Outflow of dense water from a Svalbard fjord into the Fram Strait. Deep-Sea Res. 35, 1143-1150.

Rhein, M., 1991. Ventilation rates of the Greenland and Norwegian Seas derived from distributions of the chlorofluoromethanes F11 and F12. Deep-Sea Res. 38, 485-503.

Ronski, S., Budéus. G., 2005. Time series of winter convection in the Greenland Sea, J. Geophys. Res. 110 (C04015), doi:10.1029/2004JC002318.

Rudels, B., 1986. The Θ-S relations in the northern seas: Implications for the deep circulation. Polar Res. 4, 133-159.

Rudels, B., 1987. On the mass balance of the Polar Ocean, with special emphasis on the Fram Strait. Norsk Polarinstitutt Skrifter 188, 53.

Rudels, B., Friedrich, H.J., Quadfasel, D., 1999. The Arctic Circumpolar Boundary Current. Deep-Sea Res. II 46, 1023-1062.

Rudels, B., Jones, E.P., Anderson, L.G., Kattner, G., 1994. On the intermediate depth waters of the Arctic Ocean. In: Johannessen, O.M., Muench, R.D., Overland, J.E. (Eds.), The Polar Oceans and Their Role in Shaping the Global Environment. American Geophysical Union, Washington, DC, pp. 33-46.

Rudels, B., Meincke, J., Friedrich, H., Schulze, K., 1993. Greenland Sea deep water: a report on the 1993 winter and spring cruises by RVs Polarstern and Valdivia. ICES CM 1993/C:59.

Rudels, B., Fahrbach, E., Meincke, J., Budéus, G., Eriksson, P., 2002. The East Greenland Current and its contribution to the Denmark Strait overflow. ICES Journal of Marine Science 59, 1133-1154.

Rudels, B., Björk, G., Nilsson, J., Winsor, P., Lake, I., Nohr, C., 2005. The interaction between waters from the Arctic Ocean and the Nordic Seas north of Fram Strait and along the East Greenland Current: results from the Arctic Ocean-02 Oden expedition. J. Marine Syst. 55, 1-30.

Rudels, B., Meyer, R., Fahrbach, E., Ivanov, V.V., Østerhus, S., Quadfasel, D., Schauer, U., Tverberg, V., Woodgate, R.A., 2000. Water mass distribution in Fram Strait and over the Yermak Plateau in summer 1997. Ann. Geophysicae 18, 687-705.

Schauer, U., 1995. The release of brine-enriched shelf water from Storfjord into the Norwegian Sea. J. Geophys. Res. 100, 16015-16028.

Schauer, U., Beszczynska-Möller, A., Walczowski, W., Fahrbach, E., Piechura, J., Hansen, E., 2008. Variations of measured heat flow through the Fram Strait between 1997 and 2006. In: Dickson, R.R., Meincke, J., Rhines, P. (Eds.), Arctic-Subarctic Ocean fluxes. Springer Nether-

lands, pp. 65-85.

Schlichtholz, P., Houssais, M.-N., 1999. An inverse modeling study in Fram Strait. Part II: water mass distribution and transports. Deep-Sea Res. II 46, 1083-1135.

Schlichtholz, P., Houssais, M.-N., 2002. An overview of the Θ - S correlation in Fram Strait based on the MIZEX 84 data. Oceanologia 44, 243-272.

Schlitzer, R., 2008. Ocean Data View, http://odv.awi.de.

Schlosser, P., Bönisch, G., Rhein, M., Bayer, R., 1991. Reduction of deepwater formation in the Greenland Sea during the 1980s: Evidence from tracer data. Science 251, 1054-1056.

Serreze, M.C., Holland, M.M., Stroeve, J., 2007. Perspectives on the Arctic's shrinking sea ice cover. Science 315, 1533- 1536.

Smethie, W.M. Jr., Chipman, D.W., Swift, J.H., Koltermann, K.P., 1988. Chlorofluoromethanes in the Arctic Mediterranean seas: evidence for formation of bottom water in the Eurasian basin and deep-water exchange through Fram Strait. Deep-Sea Res. 35, 347-369.

Swift, J.H., 1986. The Arctic waters. In: Hurdle, B.G. (Ed.), The Nordic Seas. Springer-Verlag, New York, pp. 129-153.

Swift, J.H., Aagaard, K., 1981. Seasonal transitions and water mass formation in the Iceland and Greenland Seas. Deep-Sea Res. 28, 1107-1129.

Swift, J.H., Koltermann, K.P., 1988. The origin of Norwegian Sea Deep Water. J. Geophys. Res. 93, 3563-3569.

Swift, J.H., Takahashi, T., Livingstone, H.D., 1983. The contribution of the Greenland and Barents Seas to the Deep Water of the Arctic Ocean. J. Geophys. Res. 88, 5981-5986.

Tanhua, T., Olsson, K.A., Jeansson, E., 2005. Formation of Denmark Strait overflow water and its hydro-chemical composition. J. Marine Syst. 57, 264-288.

Tomczak, M., 1981. A multi-parameter extension of temperature/salinity diagram techniques for the analysis of non-isopycnal mixing. Prog. Oceanogr. 10, 147-171.

Tomczak, M., Large, D.G.B., 1989. Optimum multiparameter analysis of mixing in the thermocline of the eastern Indian Ocean. J. Geophys. Res. 94, 16141-16149.

Woodgate, R.A., Aagaard, K., Muench, R.D., Gunn, J., Björk, G., Rudels, B., Roach, A.T.,

Schauer, U., 2001. The Arctic Ocean boundary current along the Eurasian slope and the adjacent Lomonosov Ridge: Water mass properties, transports and transformations from moored instruments. Deep-Sea Res. I 48, 1757-1792.